Title: The scent of survival in a warming world: how monoterpenes drive thermal adaptation in thyme

Authors: Andreas H Faber[1]*, John D. Thompson[2], Perrine Gauthier[2], Bodil Kirstine Ehlers[1].

Andreas H Faber[1],* (AHF, faberhavbro@outlook.dk, ORCiD: 0000-0003-3356-7591)

John D. Thompson[2] (JDT, john.thompson@cefe.cnrs.fr, ORCiD: 0000-0002-1600-9144)

Perrine Gauthier[2] (PG, perrine.gauthier@cefe.cnrs.fr, ORCiD: 0000-0001-7926-4647)

Bodil Kirstine Ehlers[1] (BKE, boe@ecos.au.dk, ORCiD: 0000-0002-4712-5025)

Affiliations

1: Department of Ecoscience, Aarhus University, C.F. Møllers Allé 4, 8000 Aarhus C, Denmark.

2: CEFE, CNRS, Univ. Montpellier, EPHE, IRD, 34293 Montpellier 5, France

*Contact author to whom correspondence should be addressed: faberhavbro@outlook.dk, Address: C.F. Møllers Allé 4, 8000 Aarhus C, Denmark. Phone: +4522198915

Author contributions

AHF, BKE, JDT, and PG planned and designed the research. AHF performed experiments, collected field gas-exchange data, chlorophyll fluorescence data and analysed the data. AHF, BKE, JDT and PG collected chemotype frequency data in 2024. Mortality and elevation data was collected by JT and PG. Annual temperature data from sites was collected by BKE and PG. AHF drafted the first version of the manuscript with guidance from all authors. All authors contributed to and revised the manuscript.

Funding

This work was funded by a grant from Independent Research Fund Denmark (grant number DFF-1026-00173B) to BKE.

Conflict of interest

This work has no conflict of interests.

Data availability

The data used in this manuscript will be made available on https://figshare.com upon acceptance of the manuscript for publication.

Abstract:

1 Monoterpenes are key plant secondary metabolites with well-known defensive and ecological functions, yet their role in abiotic stress tolerance remains poorly understood. In many Mediterranean plants, monoterpene composition varies markedly within and among species and is associated with climatic gradients, suggesting that these compounds may mediate plant responses to extreme heat.

2 We investigated two locally adapted ecotypes of *Thymus vulgaris* that differ in monoterpene chemistry. Phenolic ecotypes dominate shallow, rocky habitats with hot, dry summers and mild winters, whereas non-phenolic ecotypes occur in deeper soils exposed to more severe winter freezing. Although previous transplant experiments show strong local adaptation and stable geographic distributions despite high gene flow, the ecophysiological mechanisms linking monoterpene variation to climatic tolerance remain unknown.

3 We quantified heat tolerance in both ecotypes using controlled experiments that measured photosynthetic thermal limits, and combined these with field-based assessments of physiological performance, mortality, and long-term changes in ecotype composition. Using a thermal death time (TDT) framework, we predicted when each ecotype would experience photosynthetic failure under natural conditions and related these predictions to observed mortality during recent periods of intensified summer heat and drought.

4 Heat tolerance diverged between ecotypes only after heat acclimation, with the phenolic ecotype substantially increasing its thermal limits relative to the non-phenolic ecotype. This indicates that monoterpene chemistry primarily affects fitness through enhanced tolerance to extreme temperatures rather than through performance differences under benign conditions. However, despite its superior heat tolerance, the phenolic ecotype experienced elevated mortality in its warm native habitats, suggesting that recent summer temperatures may already exceed the physiological thresholds of the phenolic ecotype.

5 Synthesis. Understanding how plant functional traits mediate responses to climatic extremes is essential for predicting vegetation dynamics under climate change. Our results show that intraspecific variation in secondary chemistry can enhance physiological heat tolerance via increased acclimation capacity, yet rapid climatic warming may still overwhelm these trait-based advantages. By integrating plant chemistry, physiological thresholds, and long-term demographic changes, this study advances our understanding of how functional traits shape plant vulnerability and resilience in increasingly extreme environments

Keywords: thermal tolerance, thermal death time curve, *Thymus vulgaris*, monoterpenes, essential oils, ecotype, chemotype, functional traits, climate change

Introduction

As extreme thermal events increase in frequency, intensity, and duration at both regional and global scales (IPCC, 2023), understanding how plants respond to these changes is crucial for predicting the ecological and evolutionary impacts of climate change. The ability of species to persist under changing environmental conditions ultimately depends on their capacity to tolerate, avoid, or adapt to thermal stress. These responses are mediated by functional traits that determine physiological performance and fitness under novel or more extreme conditions. Among these, chemical traits such as the production of secondary metabolites represent a dynamic and responsive functional trait, known to affect physiological performance, survival, growth, and reproduction (Junker, 2016; Kessler & Kalske, 2018; Walker et al., 2022). Despite this ecological importance, studies that link chemical variation to plant physiological performance and then connect those physiological effects to population level outcomes over time are extremely rare (Walker et al., 2022; Endara et al., 2022).

One important class of chemical traits that exhibits striking phenotypic variation is the production of secondary compounds such as monoterpenes. In the Mediterranean region, up to 49% of the plant genera are aromatic and produce essential oils (Ross & Sombrero, 1991). Monoterpenes often make up the majority of these oils and represent a key functional trait, influencing plant interactions with herbivores, and tolerance to abiotic stresses including drought and thermal stress (Thompson, 2020). The identity and concentration of monoterpenes vary with environmental variation, both seasonally and spatially (Milos et al., 2001; Mastelić & Jerković, 2003; Keefover-Ring et al., 2014; Pratt et al., 2014; Keefover-Ring, 2022; Dodoš et al., 2024). Such variation is observed among species adapted to different environments (Ibraliu et al., 2011) and within species across environmental gradients (De Mastro et al., 2017; Dodoš et al., 2024), making monoterpenes an ideal candidate for a trait that link chemical variation to physiological performance and climate driven selection.

Monoterpene variation is particularly well documented in the *Lamiaceae* family, where many species form distinct chemotypes through polymorphism, genetically determined variants characterized by the dominance of a single monoterpene that can comprise nearly the entire essential oil profile (Sáez & Stahl-Biskup, 2002; Muñoz-Bertomeu et al., 2007; Napoli et al., 2009; Herraiz-Peñalver et al., 2013; Thompson, 2020). A striking example of monoterpene-based polymorphism occurs in wild Mediterranean thyme, *Thymus vulgaris*, which displays several distinct chemotypes, each defined by its dominant monoterpene (Granger & Passet, 1973; Vernet et al., 1986; Thompson, 2002). In Southern France, these include four non-phenolic chemotypes, dominated by either geraniol (G), α-terpineol (A), linalool (L), or thuyanol (U) and two phenolic chemotypes, dominated by either carvacrol (C) or thymol (T).

All six chemotypes co-occur at a remarkably fine spatial scale within the basin of St. Martin de Londres (43°48′N, 03°46′E), located 20 to 30 km north of Montpellier. The basin spans roughly 80 km^2 and lies within a rugged calcareous landscape, with elevations ranging from 145 m at the center to over 650 m on the surrounding hills. Although the region has a typical Mediterranean climate, with hot, dry summers and mild, damp winters, the basin is subject to frequent winter temperature inversions. When these inversions occur, cold air becomes trapped at lower elevations, leading to severe freezing events on the basin floor, while the higher slopes surrounding the basin remain comparatively mild. This sharp microclimatic contrast has produced a steep cline across just 3–5 km, with a narrow transition zone separating populations dominated by either phenolic or non-phenolic chemotypes that can be defined as two ecotypes. The phenolic ecotype (T and C) is adapted to hot, dry environments, while the non-phenolic ecotype (G, A, U, and L) is adapted to wetter lowland habitats that experience occasional severe winter freezing (Thompson et al., 2007; Thompson, 2020). In the area, the phenolic chemotypes (carvacrol and thymol) are found primarily on the higher, stony

slopes above 250 m, whereas the non-phenolic chemotypes (linalool, thuyanol-4, α-terpineol, and geraniol) are restricted to the basin floor below 200 m, where soils are deeper and historically more exposed to extreme winter freezes (Thompson, 2020). Sites consisting of mixtures of phenolic and non-phenolic chemotypes are rare, but they occur often in the elevation transition zone between 200 m and 250 m (Gouyon et al., 1986). Although gene flow between nearby phenolic and non-phenolic populations is very high, strong genetic differentiation at chemotype-associated loci suggests that local selection maintains these differences despite ongoing genetic exchange (Bataillon et al., 2022). Reciprocal transplants have confirmed the ecotypes adaptation to the different climatic condition from increased survival and growth in their respective adapted climatic environments. However, any underlying differences in the ecophysiology under thermal stress of the two ecotypes has so far not been studied. Understanding these eco-physiological responses is essential for identifying the physiological mechanisms by which climatic selection maintains the spatial distribution of phenolic and non-phenolic ecotypes. Uncovering such mechanisms is critical for predicting and understanding how traits within species my influence their capacity to persist and adapt under ongoing climate change.

In this study, we test whether differences in thermal tolerance between the phenolic and non-phenolic *T. vulgaris* ecotypes translate into differences in resilience towards heat stress in their natural environment. Our objectives are as follows. First, we generated ecotype-specific thermal death time (hereafter TDT) models that quantify how heat stress accumulates with temperature intensity and exposure duration through time (Faber et al., 2024). Second, we apply these TDT models to measured microclimate temperatures from mixed sites where the two ecotypes co-occur. This allowed us to predict the cumulative heat stress each ecotype experiences across a summer when they experience the same intensity and frequency of extreme heat events. Third, we assess how these predictions relate to differences in physiological performance and mortality levels measured in the field. Finally, we

compare these results with long-term changes in ecotype frequencies from 1970, 2010, and 2023 to assess whether changes in climate over the past five decades have altered the ecotypes relative abundance in mixed ecotype sites where both ecotypes occur. This analysis provides a demonstration of how monoterpene variation is linked to cumulative heat stress, physiological performance, mortality, and long-term ecotype shifts in *T. vulgaris*. It thus offers new insights into the mechanisms by which chemical traits influence plant populations in a warming world.

Materials and methods

Greenhouse growth conditions

Thyme seeds were collected in June 2022 in southern France from natural *T. vulgaris* populations growing in the study area of the St. Martin de Londres and stored in paper bags at room temperature until use. The seeds were collected from different sites across the area, representing multiple populations. The sites are known to contain populations in which all six chemotypes are present. In June 2023, seeds were sown in trays filled with Mediterranean peat-based soil (~5 cm layer) and kept humid under a white plastic sheet to promote germination. Once germinated, seedlings were transplanted into 2 L pots filled with a 1:1 mixture of Mediterranean peat-based soil and gravel. For each plant, one shoot tip sample (upper 2 cm) was collected and used to determine its chemotype by GC-MS (see below).

Plants were grown in the greenhouse at the Department of Ecoscience, Aarhus University, Denmark (56.198°N, 10.155°E). From December 2023 until March 2024, daily temperatures were maintained between approximately 5 and 20 °C to simulate Mediterranean winter conditions. By April 2024, all plants were flowering, and the first thermal tolerance experiment was conducted under controlled conditions, with daily temperatures ranging from ~13 to 20 °C (**Fig. S1**). Following this experiment,

greenhouse temperatures were allowed to gradually increase through the summer months. The second thermal tolerance experiment was conducted in mid-August 2024, when daily temperatures had increased to range between 25 and 35 °C (**Fig. S1**). The CO_2 concentration was maintained at ambient levels (~410 ppm), and relative humidity was kept between 40-70%. Natural sunlight was supplemented with LED lamps (Philips GreenPower LED top lighting compact, Signify N.V., Amsterdam, The Netherlands) when the photosynthetic photon flux density (PPFD) dropped below 150 µmol m^{-2} s^{-1} during the daytime, with lamps delivering up to 400 µmol m^{-2} s^{-1} PPFD at plant level. Climate conditions were controlled via an automated system (LCC4, Senmatic). Plants were watered once to twice per week and fertilized with an NPK (14:3:15) nutrient solution.

Thermal death time experiments

Thermal death time (TDT) models describe how long an organism, or its tissue, can tolerate stressful constant temperatures before reaching acute failure and succumb to the stress (Faber et al., 2024). TDT models assume that thermal damage accumulates additively through time, with fractions of damage sustained at different temperatures summing until thermal failure is reached. Because damage accumulates exponentially with temperature, the same point of failure can be reached either by short exposures to highly stressful temperatures or by longer exposures to lower stressful temperatures. Here we estimated how long each chemotype, and thus each ecotype, could withstand a range of high constant temperatures before reaching thermal failure, and used the resulting $\log_{10}$ transformed time to failure as a function of temperature, to generate TDT models for predicting thermal damage under natural fluctuating thermal conditions. The thermal tolerance experiments were generated for each chemotype during two periods: in April 2024 where all plants were flowering and temperatures resembled early spring in the Mediterranean, and again in August 2024, after plants had been exposed

191 to long-term warming in the greenhouse resembling Mediterranean summer (**Fig. S1**). Each
192 chemotype was represented in the experiments by individuals originating from at least two different
193 collection sites.

194 Thermal tolerance and thus thermal failure of the chemotypes was measured using a chlorophyll
195 fluorometer (FluorPen FP110/S; Photon Systems Instruments, Drásov, Czech Republic), specifically
196 the maximum quantum efficiency of photosystem II (F_v/F_m). The variable fluorescence (F_v) is
197 determined by subtracting the minimum fluorescence (F_0) from the maximum fluorescence (F_m) of
198 dark-adapted leaves. F_v/F_m represents the capacity of PSII to convert absorbed light into
199 photochemical energy (Berry & Bjorkman, 1980; Seemann et al., 1984; Willits & Peet, 2001; Knight
200 & Ackerly, 2002, 2003; Baker & Rosenquist, 2004). A decline in F_v/F_m of more than ~50% indicates
201 dysfunction in the photosynthetic machinery (Schreiber & Berry, 1977; Downton & Berry, 1982;
202 Knight & Ackerly, 2003; Sastry & Barua, 2017), often leading to visible tissue-level damage (Bilger
203 et al., 1984). This decline was used as a proxy for thermal failure in our experiments.

204 To determine how long the chemotypes could withstand a given constant temperature before reaching
205 thermal failure, we exposed samples to a set of constant temperatures for a range of exposure
206 durations. For each temperature, we collected five to seven independent batches, each consisting of
207 ten samples. The samples consisted of the outer tips of branches, ~2 cm in length. Ten different plants
208 per chemotype were sampled for every constant temperature tested, and for all chemotypes ten
209 different plants were represented by one sample in each batch. Sampling occurred between 07:00 and
210 10:00 h, using only healthy, fully expanded leaves of similar age.

211 After collection, samples within each batch were placed into transparent 2-mL micro centrifuge tubes
212 and kept in darkness at room temperature (20-22 °C) for 1-3 h. The batches were then illuminated
213 with ~1200 µmol photons m^{-2} s^{-1} for 30 min before being transferred to temperature-controlled water

baths. The water bath temperatures were fixed at 44, 45, 46, 47, or 48 °C in April and 44, 45, 46, 47, 48, or 49 °C in August. During heat exposure in the water baths, the samples were illuminated with ~800 µmol photons m^{-2} s^{-1}, to simulate the high light conditions that typically accompany heat stress under natural conditions. The light intensity was measured at the level of the samples in the water baths with the FluorPen enclosed in a transparent plastic bag.

For each temperature treatment, batches were removed at different exposure durations, ranging from 0 min to 24 h depending on the intensity of the temperature (see **Fig. S2** for exposure durations). The exposure durations were selected based on pilot experiments to capture the exposure duration at which F_v/F_m decreased with 50%. After the heat treatments, the batches were quickly submerged in 20 °C water for two to three minutes to rapidly decrease the temperature of the samples. The batches were then exposed to ~1200 µmol photons m^{-2} s^{-1} for 60 minutes at room temperature, and then dark adapted for 18-22 h. Subsequently, the total reduction in F_V/F_M following a stress treatment, and thus the accumulated dose of damage to PSII was estimated by measuring F_V/F_M on a single leaf on each sample. Batches measured at 0 minutes temperature exposure functioned as control samples to reflect plants at an unstressed state. For each constant temperature, we plotted F_V/F_M against exposure duration across all batches and identified the exposure duration at which F_V/F_M had decreased with 50% (see statistical data analysis further below). This threshold represents the point of thermal failure for a given temperature and was used to construct the TDT models for each chemotype.

Thermal death time predictions

To evaluate whether differences in ecotypic thermal tolerance translate into ecologically meaningful differences in stress exposure, we used TDT models to predict the rate by which each ecotype accumulates thermal damage under natural, fluctuating field conditions. To do this, we used

temperature data collected from May to September in 2015 from iButtoon Thermochron temperature loggers (Maxim Integrated, San Jose, CA, USA) placed in five different sites in the study area where both ecotypes co-occur. Instantaneous temperatures were recorded every hour within the thyme canopy to capture fine-scale variation in the thermal environment experienced by plants throughout the summer.

Using this field temperature dataset, we predicted thermal damage accumulation for each ecotype using the TDT models derived from the greenhouse experiments conducted in August 2024, when the ecotypes were most heat tolerant. Specifically, the TDT models were generated by fitting linear regression models to the $\log_{10}$-transformed time to thermal failure data plotted as a function of temperature for the two ecotypes. These regressions yielded the slope (β) and intercept (α) parameters for each ecotype, which were then used to predict the duration of tolerable thermal exposure in the field according to the following equation (Jørgensen et al., 2021):

$$\text{Accumulated damage} = \sum_{i=1}^{n} \frac{100 \cdot (t_{i+1} - t_i)}{10^{(\beta \cdot \max(T_i; T_{i+1}) + \alpha)}} \qquad \text{(Eqn. 1)}$$

Where accumulated damage is calculated over each time interval i unit t_e which is the time interval for which the total accumulated damage is calculated. The β and α are the slope and intercept of the TDT model, respectively. The denominator is the fraction of the tolerable exposure duration for the maximum temperature (of T_i and T_{i+1}) in each time interval. To calculate damage accumulation, we linearly interpolated temperature between consecutive recorded values. Specifically, temperatures were interpolated at one-minute intervals between each pair of successive hourly measurements (T_i and T_{i+1}), assuming a linear change in temperature over time. Thermal damage was then calculated on a minute-by-minute basis using the interpolated temperatures and summed across each hourly

interval and over the full timeseries. Damage accumulation was only calculated for temperatures exceeding the threshold at which each ecotype experienced thermal failure after 24 hours of exposure according to Jørgensen et al., 2022. Here 100% damage corresponds to the point at which F_v/F_m decreases by 50%.

As natural stressful heat events only occur periodically and primarily during daytime, plants are expected to repair at least some fraction of accumulated damage during cooler night periods and days with non-stressful temperatures. Without incorporating any recovery, our models would predict that a single extreme heat event could drive plants to complete thermal failure which would potentially mask differences between ecotypes under many repeated natural heat events. By introducing a set of low nighttime recovery scenarios, we were able to examine how quickly ecotypes accumulate damage toward the 100% failure threshold under more plausible sequences of heat exposure during the summer, while still allowing cumulative damage to build when heat events occur frequently. Although the true recovery rates of the ecotypes are unknown, examining several conservative scenarios provides a more nuanced assessment of whether heat events are sufficiently intense and frequent to generate ecotypic differences in thermal stress. We modelled four nighttime recovery scenarios (0%, 5%, 10%, and 15% of daytime accumulated damage), under the assumption that recovery is no longer possible once damage reaches 100%. This means for example that a 5% recovery rate applied to 50% damage accumulated during the day would reduce the total damage to 45% by the following morning. These damage accumulation predictions are based on microclimate air temperatures rather than direct leaf temperatures, which may potentially under- or overestimate the actual thermal load experienced by the plants. While this limits the accuracy of absolute damage estimates, both ecotypes experience the same microclimatic conditions, so any bias should affect

283 them similarly. The predictions therefore still offer a meaningful comparative assessment of potential
284 ecotypic differences in thermal stress exposure.
285
286 **Field gas-exchange and fluorescence measurements**
287 Gas-exchange measurements were conducted in June 2024 between approximately 11:00 and 17:00
288 using a Li-Cor 6800 portable photosynthesis system (Li-Cor, Lincoln, NE, USA) equipped with a
289 clear-top conifer chamber, allowing ambient light to serve as the light source during measurements.
290 Measurements were carried out at four field sites: two mixed sites, where phenolic and non-phenolic
291 ecotypes were present, one site dominated by the phenolic ecotype, and one site dominated by the
292 non-phenolic ecotype.
293
294 For each measurement, a leaf temperature on a selected branch exposed directly to the sun was first
295 recorded using a thermocouple attached to the Li-Cor. The conifer chamber was then clamped onto a
296 branch, and leaf temperature within the chamber was controlled using energy balance to match the
297 recorded pre-clamp leaf temperature as closely as possible during the measurements. After a 2-minute
298 stabilisation period to allow the gas exchange system and physiological parameters to reach steady
299 state, net photosynthesis (A_{net}, CO_2 m^{-2} s^{-1}) and transpiration (E, mmol H_2O m^{-2} s^{-1}) were measured.
300 Immediately after, the chamber was darkened, and after 3 minutes in darkness, dark respiration (R_{Dark},
301 CO_2 m^{-2} s^{-1}) was measured according to Bruhn et al., (2025). The Li-Cor was operated using
302 the "conifer" geometry setting to account for the 3D like leaf morphology of the *T. vulgaris* branches.
303 The measurements were conducted with a relative humidity of ~ 60%, a flow rate of 400 µmol s^{-1}, a
304 fan speed of 10.000 rpm and a CO_2 concentration of 410 ppm in the conifer chamber. Measurements
305 were conducted diurnally on 10 individual plants per site. At each of the mixed sites, five phenolic
306 and five non-phenolic individuals were measured per day over two consecutive days. Throughout the

day, all 10 plants were measured in chronological order (from plant 1 to 10) and this sequence was repeated multiple times, resulting in approximately four to seven repeated measurements per plant per day. Ecotypes were alternated within the measurement order to avoid systematic time-of-day effects between measurements of phenolic and non-phenolic.

Chlorophyll fluorescence measurements were performed using a FluorPen on the same individual plants on which gas-exchange measurements were conducted to assess the maximum (F_v/F_m) and effective (F_v'/F_m') quantum yields of photosystem II. F_v/F_m was measured in situ on dark-adapted leaves following dark adaptation for 40–50 minutes before measurement. The leaves were dark-adapted using leaf clips gently secured with rubber bands. F_v'/F_m' was measured on fully light-exposed leaves. For both F_v/F_m and F_v'/F_m', one measurement per plant was taken during the same diurnal measurement period as gas-exchange, ensuring consistency in environmental conditions across datasets.

Field mortality survey

We quantified plant mortality in the field in late autumn (November) 2024 after several years of intense and prolonged summer drought and increasing extreme temperature conditions (**Fig. 1**). The study was based on the same subset of populations (see above) in and around the basin of St. Martin de Londres where chemotype composition has been observed in the early 1970s (Vernet et al., 1977) and again in 2009–2010 (Thompson et al., 2013). This subset of populations involved six transects place in a circular manner around the basin extending from phenolic to non-phenolic populations. Each transect had six sites, two sites that were 100% phenolic chemotypes in the 1970s, two mixed sites and two 100% non-phenolic chemotypes at that time. in each site we quantified four categories of plants: (i) plants with no sign of dried branches and stems, (ii) plants with < 30% of dried branches

and stems, (iii) plants with > 30% of dried branches, and most often ca. ⅔ or ¾ of dried branches and stems, (iv) plants with 100% dried branches and stems. For the latter the stems could be pulled out of the ground and pallets appeared to have died.

Ecotype frequency estimation

In 2024, we resampled a subset of populations in and around the basin of St. Martin de Londres from which the chemotype composition had been observed in the early 1970s (Vernet et al., 1977) and again in 2009–2010 (Thompson et al., 2013). Populations were sampled with GPS accuracy based on the 2009/2010 sampling. At each site, we sampled fresh leaves from 30 random thyme plants. Fresh shoot tips (upper 2 cm) were placed in eppendorf tubes containing 98 % ethanol, placed in a cooling box until returned to the lab where they were stored at 5 °C until analysis.

Ecotype estimation with GCMS

The ecotype and chemotype identities of the plants on which gas-exchange and chlorophyll fluorescence measurements were conducted were determined using gas chromatography–mass spectrometry (GC-MS) based on the monoterpene profiles of fresh leaf tissue samples stored at 5 degrees C in 98% ethanol. Prior to GC-MS, extracts were diluted in methanol at a 1:4 ratio. Chemical analysis was performed using a Shimadzu GCMS-QP2101Plus fitted with an Omegawax 320 column (30 m × 0.25 mm; 0.25 μm film thickness), with helium as the carrier gas. Monoterpene compounds were identified by comparing retention times and mass spectra to reference standards in a spectral library. Based on the identity of the dominant monoterpenes, each plant had its chemotypes identified and classified into a phenolic (carvacrol, thymol) or non-phenolic (α-terpineol, geraniol, thuyanol, linalool) ecotype.

355 **Statistical analysis**

356 Generalized additive models (GAMs) were used to estimate the decrease in F_v/F_m following the stress
357 treatments and determine the time point which F_v/F_m decreased with 50%. For each constant
358 temperature treatment, GAMs were fitted to measurements of F_v/F_m as a function of stress duration,
359 using automated smoothness selection in the *mgcv* library in R v.4.1.0 (R Core Team, 2021) and
360 restricted maximum likelihood (REML) (Wood, 2017). Individual plants were included as a random
361 effect in the models. The GAMs had the following components:
362
363 $$y_i = \alpha + f(x_i) + \varepsilon_i \qquad \text{(Eqn. 2)}$$
364
365 Where y_i is the observation at the time x_i, α is the intercept, $f(x_i)$ is a smooth function and ε_i is the
366 residual error. This approach makes no *a priori* assumption about the functional relationship between
367 variables (Wood, 2017), allowing a depiction of F_v/F_m over exposure duration. The fitted GAMs were
368 then used to identify the time point at which F_v/F_m decreased with 50% for each stress assay. The
369 estimated time points of thermal failure, along with the fitted GAMs, are presented in the
370 supplementary material (**Fig. S2**).

371 To evaluate whether the TDT models differed significantly between the ecotypes, we compared two
372 linear models predicting $\log_{10}$-transformed time to thermal failure as a function of temperature: one
373 including an interaction term between ecotype and temperature, and one without the interaction. The
374 best model was evaluated using the Akaike's Information Criterion (AIC). From the fitted TDT model
375 parameters (slope and intercept), we calculated CT_{max}, defined here as the temperature at which
376 thermal failure occurs after 1 hour of exposure, and Q_{10}, which represents the factor by which the rate
377 of thermal failure changes with every 10 °C change in temperature. These allowed us to compare not
378 only the absolute thermal limits (CT_{max}) but also the thermal sensitivity (Q_{10}) between ecotypes. For

physiological parameters measured in the field (gas-exchange and chlorophyll fluorescence), mortality rates, and site altitudes, we conducted two-way ANOVAs to test for differences between ecotypes and sites. Significant effects were further examined using Tukey's post-hoc tests to identify pairwise differences.

Results

Thermal death time predictions for phenolic and non-phenolic ecotypes

TDT models were first generated in April 2024, when all plants were flowering and acclimated to relatively cool temperatures (~13–20 °C). These models were used to derive CT_{max} estimates (the temperature causing mortality after 1 hour of exposure) and Q_{10} values, which represent the factor by which mortality increases for every 10 °C increase in temperature. At this stage, thermal tolerance levels were similar across all six chemotypes, with an average Q_{10} of 26,864 and a predicted CT_{max} of 45.95 °C (dotted lines in **Fig. 1**).

Three months later, after plants had gradually acclimated to summer greenhouse conditions (~25–35 °C), thermal tolerance had increased substantially (solid lines in **Fig. 1**). At this stage phenolic chemotypes (carvacrol and thymol) were more heat tolerant than non-phenolic chemotypes. Phenolic chemotypes had an average Q_{10} of 235 and a CT_{max} of 49.91 °C, whereas non-phenolic chemotypes had a Q_{10} of 3115 and a CT_{max} of 47.91 °C. This pattern was supported by TDT model comparisons: including ecotype as an interaction term with temperature significantly improved model fit ($\Delta AIC = 46.8$), showing that phenolic and non-phenolic ecotypes differed significantly in thermal tolerance.

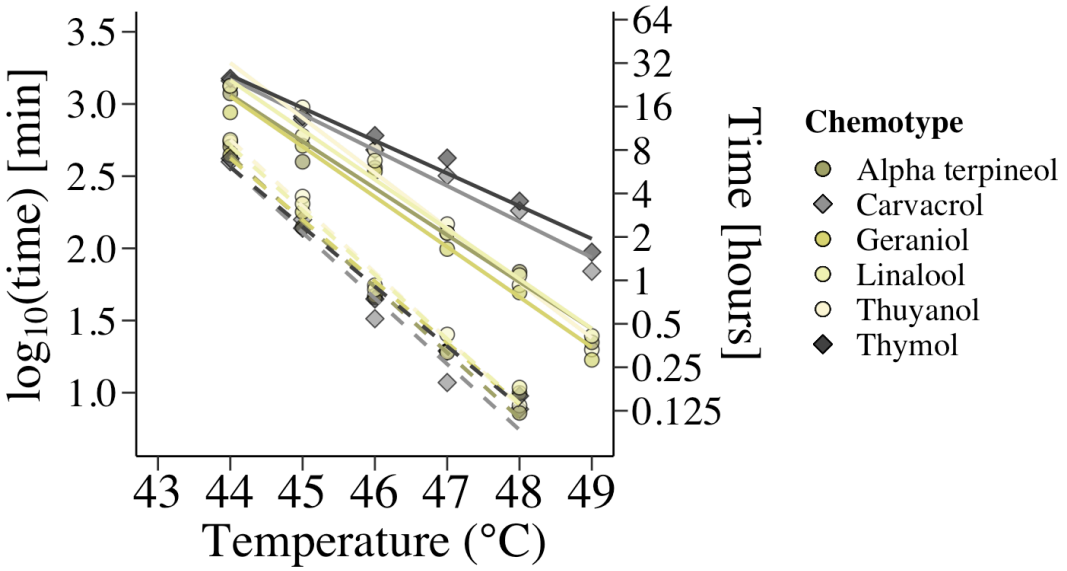

Figure 1. Thermal death time (TDT) models for six chemotypes of *Thymus vulgaris*. The y-axis shows the $\log_{10}$-transformed time (minutes) to thermal failure, the x-axis shows the treatment temperature (°C) and the third axis shows the time to thermal failure in hours. All plants were grown in a greenhouse and were approximately one year old at the time of measurement. The dotted lines represent TDT models based on measurements taken in April, when plants were acclimated to cooler conditions (~13–20 °C), while solid lines represent models from August, when plants were heat-acclimated to warmer temperatures (~25–35 °C). The TDT models represent the time to thermal failure at different temperatures where thermal failure was defined as a 50% decline in F_v/F_m, indicating significant failure of photosynthetic efficiency. The six chemotypes include linalool, alpha-terpineol, thuyanol, and geraniol, which are classified as non-phenolic ecotypes (yellow symbols and lines) adapted to cooler, wetter environments, and carvacrol and thymol, which are phenolic ecotypes (dark symbols and lines) adapted to warmer, more arid climates.

To assess how differences in thermal tolerance, as represented by the TDT models, translate into differences in the ecotypes' ability to withstand extreme heat in natural conditions, we used ecotype-specific TDT predictions to estimate when photosynthetic thermal failure occurred during the 2015 growing season in mixed populations of *T. vulgaris* from the St. Martin de Londres basin. Using hourly microclimatic temperature data recorded in situ from May to November at mixed sites where both ecotypes co-occur, we modelled cumulative thermal damage for each ecotype across five different sites. We modelled four nighttime recovery scenarios (0%, 5%, 10%, and 15%) to represent

varying capacities for stress recovery. At 0% recovery, mortality is likely to occur after a single or few extreme temperature events, whereas higher recovery rates mean that multiple consecutive extreme events are needed to reach lethal damage. This framework allows a more nuanced comparative assessment of how both the frequency and severity of heat stress episodes affect stress levels among the ecotypes.

Across all recovery scenarios and sites, the phenolic ecotype consistently reached photosynthetic thermal failure later in the summer compared to the non-phenolic ecotype (**Fig. 2A**), supporting its greater heat tolerance observed under controlled conditions. Furthermore, complete failure (i.e., 100% damage under all four recovery scenarios) occurred at only one site for the phenolic ecotype, while two sites showed complete failure for the non-phenolic ecotype regardless of the recovery rate. Notably, the relative abundance of the two ecotypes at sites where they both co-occur has shifted since 1970, with the phenolic ecotype increasing in frequency across all mixed sites (**Fig. 2B**). This is the first evidence combining controlled experiments and field studies of natural temperature variation showing that the phenolic ecotype is less vulnerable to extreme heat stress in habitats where it co-occurs with the non-phenolic ecotype.

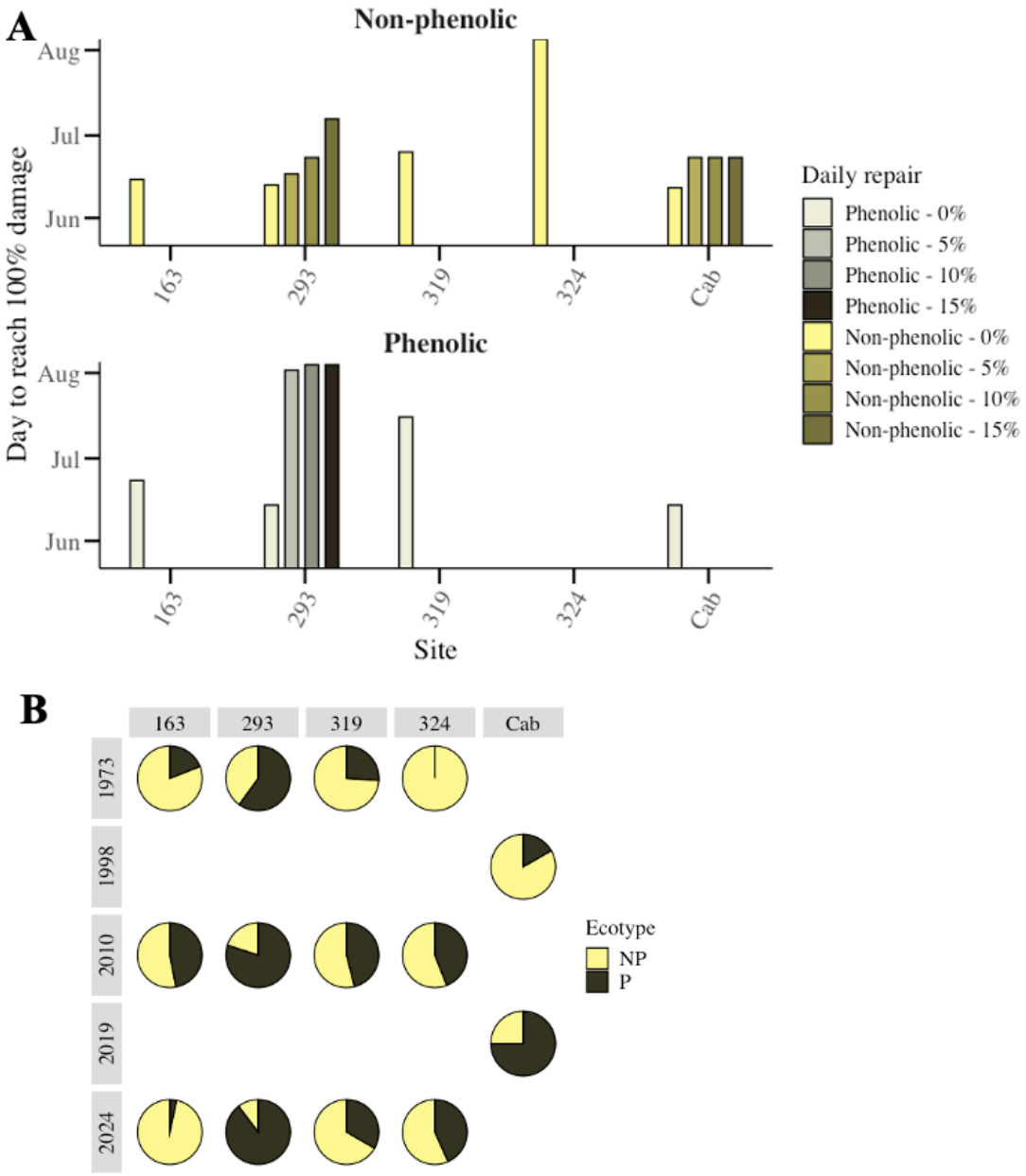

435

436 **Figure 2. A**) Predicted timing of photosynthetic thermal failure (i.e., 100% damage accumulation) for phenolic and non-
437 phenolic *Thymus vulgaris* ecotypes within mixed sites, sites where phenolic and non-phenolic individuals occur in
438 roughly equal proportions, in the basin of St. Martin de Londres. Predictions are based ecotype specific thermal death
439 time models using hourly microclimatic temperature data recorded by thermologgers placed within the thyme vegetation
440 from May to November 2023. For each ecotype, four damage scenarios are shown, assuming different rates of daily
441 recovery: 0%, 5%, 10%, or 15%. These values represent the proportion of accumulated damage that is repaired overnight
442 (e.g., 50% accumulated damage would be reduced to 35% with 15% recovery). Recovery is assumed to stop once 100%

damage is reached. The y-axis indicates the day when 100% damage accumulated across days during the summer, and the x-axis shows the identity of each site. The pie-charts (**B**) illustrate the frequency of phenolic (black), and non-phenolic (yellow) ecotypes sampled in 1970, 2010 and 2024 on the sites.

Physiological performance and mortality levels

To assess ecotype-level physiological performance under summer field conditions, we measured midday gas-exchange and chlorophyll fluorescence across phenolic, non-phenolic, and mixed *T. vulgaris* populations in June 2024 (**Fig. S3**). Physiological parameters included leaf net photosynthesis, dark respiration, transpiration, and both maximum (F_v/F_m) and effective (F_v'/F_m') quantum efficiency of photosystem II.

Across mixed sites, where both ecotypes co-occur, phenolic and non-phenolic plants did not differ significantly in any measured trait, indicating similar physiological functioning. However, when comparing individuals across different site types, phenolic individuals growing in phenolic-dominated sites showed significantly higher F_v/F_m ($P < 0.05$, $F = 12.38$) and F_v'/F_m ($P < 0.05$, $F = 16.3$) values than non-phenolic individuals in non-phenolic sites.

Mortality surveys conducted late in 2024 revealed differences among site types in longterm stress levels (**Fig. 3A**). Individuals in phenolic-dominated sites exhibited the highest proportion of whole-plant death. Mortality was significantly higher in "pure" phenolic sites compared to mixed sites (difference = 5.37%, 95% CI: 0.61 - 10.12, $P_{adj} < 0.05$), but not significantly different from non-phenolic sites ($P_{adj} > 0.05$). The warmer phenolic sites are located at significantly higher elevations than mixed sites (difference = 54.3 m, 95% CI: 13.1 to 95.5 m, $P_{adj} < 0.05$), indicating a strong association between chemotype composition and elevation across the study area (**Fig. 3B**). While phenolic sites were also, on average, 57.9 m higher than non-phenolic sites, this difference was not statistically significant (95% CI: –1.5 to 117.4 m, $P_{adj} > 0.05$). No significant difference in elevation

was observed between non-phenolic and mixed sites (difference = –3.6 m, 95% CI: –61.7 to 54.5 m, $P_{adj} > 0.05$).

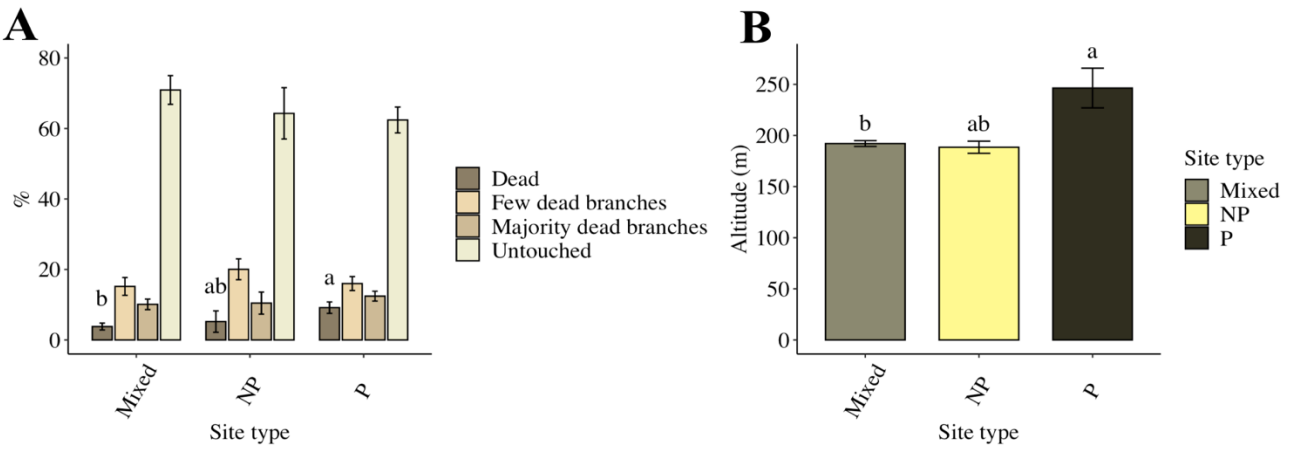

Figure 3. A) Proportion (%) of *Thymus vulgaris* individuals measured in 2024 across site types in the basin of St. Martin de Londres, southern France. Sites were categorized into site types based on whether the *Thymus vulgaris* population was predominantly phenolic, non-phenolic, or mixed (i.e., roughly equal proportions of phenolic and non-phenolic individuals). Individuals were classified into four categories based on branch condition: Untouched, few dead branches, majority dead branches, and dead. The x-axis shows site types. **B**) Altitude (meters) of the same sites grouped by site type shown on the x-axis. Altitude data are summarized per site type. Groups labelled with different letters are significantly different ($P < 0.05$), while groups sharing the same letter are not ($P > 0.05$).

Discussion

Monoterpenes as a functional trait that increases heat tolerance.

This study provides novel insight in to how monoterpenes contribute to plant thermal tolerance, with their effects depending both on the identity of the monoterpene and the environmental context in which plants are exposed to heat stress. Previous reciprocal transplant experiments have provided evidence that the phenolic *T. vulgaris* ecotype is better at surviving warm and dry summers compared to the non-phenolic ecotype which better survives extreme cold winter temperatures (Amiot et al

2005; Thompson et al., 2007). Together with evidence showing that the phenolic ecotype is known to occur more frequently in hotter, drier environments than the non-phenolic ecotype (Bataillon et al., 2022; Faber et al., 2025), this supports the hypothesis that differences in monoterpene profiles contribute directly to enhanced thermal resilience. However, until now it has remained unclear whether this pattern reflects an intrinsic physiological advantage in coping with high temperatures and what the mechanism underlying this advantage might be.

Here we demonstrate that variation in dominant monoterpene (i.e. phenolic or non-phenolic) act as a functional trait affecting the duration that photosynthetic machinery can withstand heat stress. Both ecotypes in this study showed high thermal sensitivity when acclimated to modest spring temperatures at flowering stage, with photosynthetic failure rates increasing by approximately 2.77-fold for every 1 °C increase in temperature and CT_{max} values around 45.95 °C. However, after long-term acclimation to higher temperatures, thermal sensitivity decreased markedly for both ecotypes, with failure rates increasing by a factor of about 1.73 per 1 °C increase for the phenolic ecotype and 2.23 per 1 °C increase for the non-phenolic ecotype. At this stage, the phenolic ecotype showed a larger increase in CT_{max} (~4 °C), reaching nearly 50 °C, while the non-phenolic ecotype plateaued at ~48 °C. These results suggests that monoterpenes not only increase the duration plants can sustain extreme temperatures, but also that this increase in resistance to accelerating damage rates seems to manifest through acclimation to more extreme temperatures, with the phenolic monoterpenes showing a markedly stronger reaction than the non-phenolic.

We found no significant differences between phenolic and non-phenolic ecotypes when measured under field conditions at the mixed sites, including net photosynthesis, transpiration, and dark respiration, chlorophyll fluorescence measurements. Hence, at our time of field measure (June 2024) heat or water stress may not have been intense enough to reveal any ecotypic differences in

physiological performance. Taken together, although monoterpenes, are linked to increased thermal tolerance, their physiological effects seem to be conditional and appear to become functionally important when heat stress intensifies, and plants undergo acclimation responses.

To assess whether the physiological differences observed under controlled conditions are relevant in natural environments, we applied ecotype specific TDT models to estimate the timing of photosynthetic thermal failure during the 2015 growing season in mixed populations of *T. vulgaris* in the St. Martin de Londres basin. Using measured microclimatic air temperatures, this approach provides a comparative framework to evaluate differences in the timing of photosynthetic failure between ecotypes under natural temperature fluctuations. Across all sites and prediction scenarios, the phenolic ecotype consistently reached photosynthetic failure later in the season than the non-phenolic ecotype (**Fig. 2A**), suggesting greater resilience to repeated thermal stress. *T. vulgaris* can commonly shed a substantial proportion of its leaves during the summer drought.

It is commonly known that *T. vulgaris* sheds a substantial proportion of its leaves during the summer drought. Since the damage accumulation predictions in this study are based on thermal failure of leaf photosynthesis, these predictions may be more directly related to the timing of this phenological transition and thus more indirectly related to field mortality levels. The point at which cumulative damage reaches critical levels in natural settings could thus coincide with the onset of leaf shedding. Earlier or more frequent shedding in response to thermal stress may represent a protective response, but is also likely to reduce the plant's carbon gain over the season. Over time, this could potentially lead to reduced growth, reproduction, and long-term survival, especially for the non-phenolic ecotype that has lower thermal tolerance and is more likely to experience photosynthetic failure earlier in the summer.

Beyond their established ecological functions in defence, allelopathy, and neighbour interactions (Ehlers & Thompson, 2004; McCormick et al., 2012; Effah et al., 2019; Su et al., 2023), growing evidence suggests that monoterpenes also contribute to abiotic stress tolerance, particularly under heat and drought. Experimental studies show that monoterpenes can stabilise cellular membranes, limit oxidative damage, and scavenge reactive oxygen species (Sharkey & Singsaas, 1995; Loreto et al., 1998; Loreto & Velikova, 2001; Zuo et al., 2017; Xu et al., 2022). In fumigation experiments, monoterpenes have been shown to activate stress-responsive transcription factors, reduce ROS accumulation, and maintain photosynthetic efficiency under both heat and cold stress (Riedlmeier et al., 2017; Wenig et al., 2019; Zhao et al. 2020). While the specific mechanisms remain to be identified, it is clear that different monoterpenes vary in their protective capacity (Godard et al., 2008; Riedlmeier et al., 2017; Wenig et al., 2019; Zielińska-Błajet et al., 2020). Phenolic monoterpenes are known for their strong antioxidant activity and have been shown to interact more strongly with membranes and with higher membrane partitioning effects than non-phenolic compounds, especially under dehydrating stress (Pham et al. 2015). These properties likely reflect the greater thermal tolerance observed in phenolic ecotypes in our study and may help explain their prevalence in hotter, drier habitats.

While previous studies have shown that monoterpenes can improve plant heat tolerance (Kesselmeier & Staudt, 1999; Holopainen & Blande, 2013; Zuo et al., 2017; Tian et al., 2020), these studies do not assess thermal tolerance in a way that distinguishes whether these effects result solely by the monoterpenes presence or from a combination of monoterpenes and induced acclimation or hardening processes. In this study, the TDT models reflect the plants' thermal limits for their physiological state at the time of testing, likely without further hardening or acclimation during heat exposure (Ørsted et al., 2022; Faber et al., 2024). Because phenolic and non-phenolic ecotypes showed similar heat tolerance before acclimation but diverged markedly after long-term exposure to high sub-lethal

temperatures, our results suggest that monoterpenes may increase thermal tolerance through an interaction with acclimation and/or hardening mechanisms. Future studies should test this hypothesis more directly, e.g. by using the TDT framework to compare plants that produce monoterpenes with non-producing plants under both constant and variable heat exposure protocols. If monoterpene producing plants consistently demonstrate higher tolerance under conditions that promote acclimation and/or hardening, this would show that monoterpenes enhance heat tolerance by interacting with these physiological responses, rather than by increasing thermal tolerance solely through their presence. Simultaneous measures of hardening markers such as heat shock proteins could provide further insights into the mechanisms underlying enhanced thermal tolerance.

Historic and future ecotype frequencies: towards a phenolic garrigue?

Historically, *T. vulgaris* populations inside, the basin of St. Martin de Londres where there is a temperature inversion have primarily been non-phenolic (Thompson et al., 2013). However, winter freezing below -15 °C, temperatures that cause severe mortality of phenolic but not of non-phenolic chemotypes (Amiot et al., 2005) has not occurred since 1987 (**Fig. 4A**) and we are already seeing a corresponding change in the distribution of ecotypes (Thompson et al., 2013). Since 1970, mixed ecotype populations have increased in the relative abundance of the phenolic ecotype, with two populations becoming exclusively phenolic. In contrast, populations that have historically been phenolic have remained stable. However, in this study we see a new trend emerging with intensifying summer drought and rising temperatures over that last ~ 8 years (**Fig. 4B,C**). While the phenolic ecotype is associated with hotter, drier environments (Thompson et al., 2007; Thompson, 2020), and as shown here, have higher heat stress tolerance, we now observe signs of elevated mortality levels within phenolic populations. Phenolic populations are usually found outside and at the rim of the basin of St. Martin de Londres at higher altitudes (**Fig. 3B**), outside of the temperature inversion,

580 where summer temperatures are higher (**Fig. 4B**). This suggests that although phenolic monoterpenes
581 confer an adaptive advantage under heat stress, these traits alone may not be sufficient if climate
582 extremes continue to intensify. This raises questions about the future viability of phenolic populations
583 in some of their current sites.
584

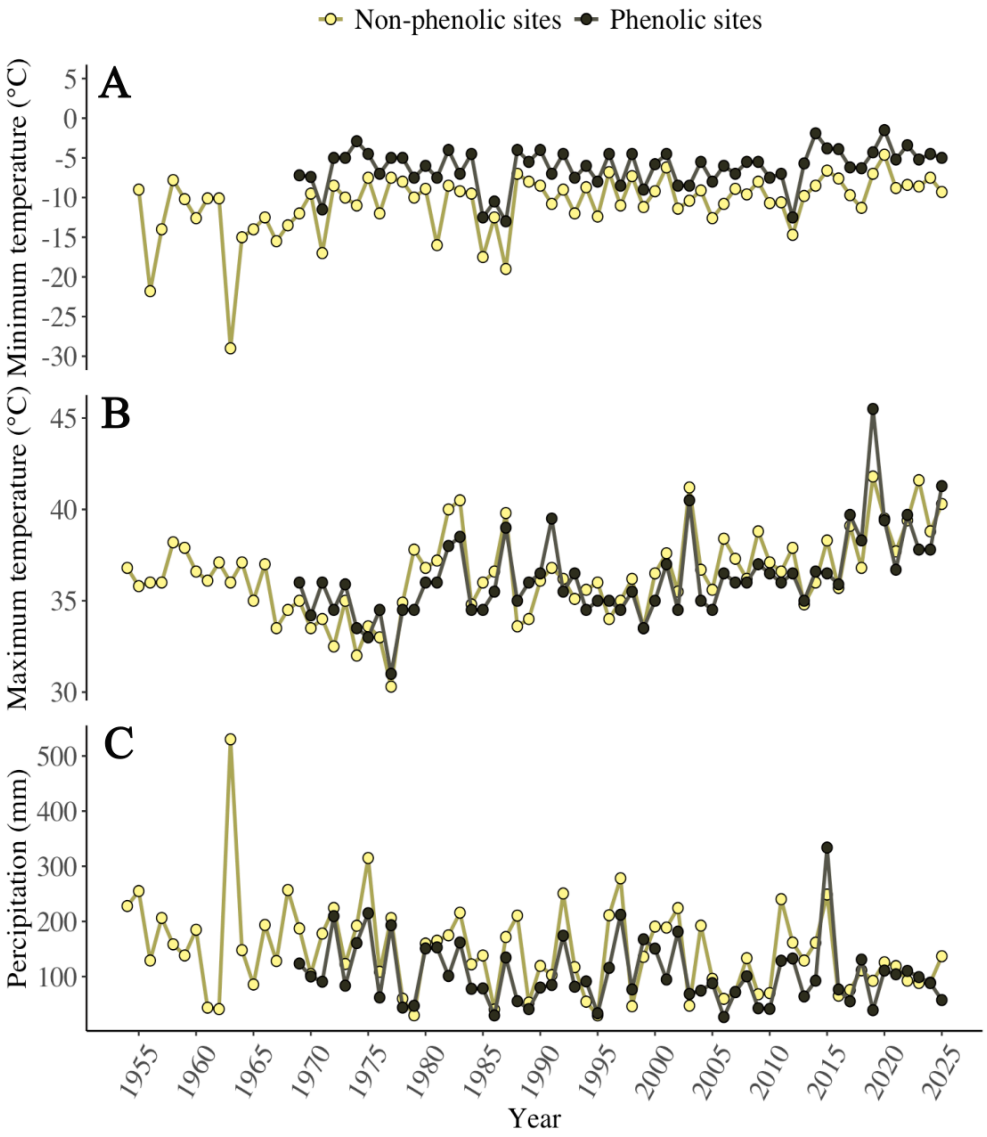

585
586 **Figure 4.** Annual climate trends for areas dominated by either phenolic (black symbols) or non-phenolic (yellow symbols)
587 plant populations in southern France, based on climate records from Montpellier and St. Martin de Londres climate
588 stations from 1954 to 2025. **A**) Minimum annual temperature (°C) at phenolic and non-phenolic sites. **B**) maximum annual

temperature (°C), showing consistently higher values at phenolic sites compared to the basin. **C**) Total summer precipitation (mm; June-August) recorded each year at non-phenolic sites.

Taken as a whole, the long-term ecotypic population and warming climate trends combined with the TDT predictions, physiological performance and field mortality levels of the ecotypes suggest that differences in heat stress tolerance have contributed to the observed ecotype shifts in *T. vulgaris*. These results establish a direct physiological link that underlies the long-term increase in phenolic ecotype frequency and demonstrates how secondary compounds such as monoterpenes alter thermal tolerance and consequently shape population dynamics under a warming climate.

Finally, multiple observations (Thompson, 2020) and recent findings by Faber et al. (2025) show that ecotypic variation in monoterpene composition occurs across other several regions of the Mediterranean. In our study species, phenolic ecotypes have begun to expand into areas historically dominated by non-phenolic plants (Thompson et al., 2013), which is not surprising given the high levels of genetic exchange between populations (Bataillon et al., 2022). Such shifts in the spatial distribution of ecotypes may have long-term consequences for community composition and ecosystem functioning, given the central role monoterpenes play in plant–plant and plant–herbivore interactions (Ehlers & Thompson, 2004; McCormick et al., 2012; Holopainen & Blande, 2013; Ehlers et al., 2014). The Mediterranean garrigue-type habitat may well become increasingly dominated by phenolic ecotypes, with corresponding effects on biotic interactions and ecosystem functioning.

614 **Literature**

615 Amiot, J., Salmon, Y., Collin, C., & Thompson, J. D. (2005). Differential resistance to freezing and
616 spatial distribution in a chemically polymorphic plant Thymus vulgaris. *Ecology Letters*, *8*(4), 370-
617 377.
618
619 Baker, N. R., & Rosenqvist, E. (2004). Applications of chlorophyll fluorescence can improve crop
620 production strategies: an examination of future possibilities. *Journal of experimental*
621 *botany*, *55*(403), 1607-1621.
622
623 Bataillon, T., Gauthier, P., Villesen, P., Santoni, S., Thompson, J. D., & Ehlers, B. K. (2022). From
624 genotype to phenotype: Genetic redundancy and the maintenance of an adaptive polymorphism in the
625 context of high gene flow. *Evolution Letters*, *6*(2), 189-202.
626
627 Berry, J., & Bjorkman, O. (1980). Photosynthetic response and adaptation to temperature in higher
628 plants. *Annual Review of plant physiology*, *31*(1), 491-543.
629
630 Bilger, H, W., Schreiber, U., Lange, O. (1984). Determination of leaf heat resistance: comparative
631 investigation of chlorophyll fluorescence changes and tissue necrosis methods. *Oecologia*, 63, 256–
632 262.
633
634 Bruhn, D., Griffin, K. L., & Møller, I. M. (2025). Importance of Timing of Dark Acclimation for
635 Estimating Light Inhibition of Leaf Respiratory CO2 Efflux. *Plant, Cell & Environment*, *48*(5), 3151-
636 3158.
637

638 Schreiber, U., & Berry, J.A. (1977). Heat-induced changes of chlorophyll fluorescence in intact
639 leaves correlated with damage of the photosynthetic apparatus. Planta. 136: 233–238.
640
641 De Mastro, G., Tarraf, W., Verdini, L., Brunetti, G., & Ruta, C. (2017). Essential oil diversity of
642 Origanum vulgare L. populations from Southern Italy. *Food chemistry*, *235*, 1-6.
643
644 Dodoš, T., Novaković, J., Vujisić, L., Marin, P. D., & Rajčević, N. (2024). Geographic variability of
645 winter savory essential oil. *Industrial Crops and Products*, *210*, 118167.
646
647 Downton, W. J. S., & Berry, J. A. (1982). Chlorophyll fluorescence at high temperature. Biochim
648 Biophys Acta. 679: 474–478.
649
650 Effah, E., Holopainen, J. K., & McCormick, A. C. (2019). Potential roles of volatile organic
651 compounds in plant competition. *Perspectives in Plant Ecology, Evolution and Systematics*, *38*, 58-
652 63.
653
654 Ehlers, B. K., Charpentier, A., & Grøndahl, E. (2014). An allelopathic plant facilitates species
655 richness in the M editerranean garrigue. *Journal of Ecology*, *102*(1), 176-185.
656
657 Ehlers, B. K., & Thompson, J. (2004). Do co-occurring plant species adapt to one another? The
658 response of Bromus erectus to the presence of different Thymus vulgaris
659 chemotypes. *Oecologia*, *141*(3), 511-518.
660

661 Endara, M. J., Soule, A. J., Forrister, D. L., Dexter, K. G., Pennington, R. T., Nicholls, J. A., ... &
662 Coley, P. D. (2022). The role of plant secondary metabolites in shaping regional and local plant
663 community assembly. *Journal of Ecology*, *110*(1), 34-45.
664
665 Faber, A. H., Bataillon, T., & Ehlers, B. (2025). Climate-driven convergence of chemical ecotypes in
666 Mediterranean Lamiaceae. *Authorea Preprints*.
667
668 Faber, A. H., Ørsted, M., & Ehlers, B. K. (2024). Application of the thermal death time model in
669 predicting thermal damage accumulation in plants. *Journal of Experimental Botany*, *75*(11), 3467-
670 3482.
671
672 Godard, K. A., White, R., & Bohlmann, J. (2008). Monoterpene-induced molecular responses in
673 Arabidopsis thaliana. *Phytochemistry*, *69*(9), 1838-1849.
674
675 Gouyon, P. H., Vernet, P., Guillerm, J. L., & Valdeyron, G. (1986). Polymorphisms and environment:
676 the adaptive value of the oil polymorphisms in Thymus vulgaris L. *Heredity*, *57*(1), 59-66.
677
678 Granger, R., & Passet, J. (1973). Thymus vulgaris spontane de France: Races chimiques et
679 chemotaxonomie. *Phytochemistry*, *12*(7), 1683-1691.
680
681 Herraiz-Peñalver, D., Cases, M. Á., Varela, F., Navarrete, P., Sánchez-Vioque, R., & Usano-
682 Alemany, J. (2013). Chemical characterization of Lavandula latifolia Medik. essential oil from
683 Spanish wild populations. *Biochemical systematics and ecology*, *46*, 59-68.
684

685 Holopainen, J. K., & Blande, J. D. (2013). Where do herbivore-induced plant volatiles go?. *Frontiers*
686 *in plant science*, *4*, 185.
687
688 Ibraliu, A., Mi, X., Ristic, M., Stefanovic, Z. D., & Shehu, J. (2011). Analysis of essential oils of
689 three wild medicinal plants in Albania. *Journal of Medicinal Plants Research*, *5*(1), 58-62.
690
691 IPCC. (2023) In: Core Writing Team, H. Lee & J. Romero (Eds) *Climate change 2023: synthesis*
692 *report. Contribution of Working Groups I, II and III to the sixth assessment report of the*
693 *Intergovernmental Panel on Climate Change. Geneva,* Switzerland: IPCC, PP. 35-115.
694
695 Junker, R. R. (2016). Multifunctional and diverse floral scents mediate biotic interactions embedded
696 in communities. In *Deciphering chemical language of plant communication* (pp. 257-282). Cham:
697 Springer International Publishing.
698
699 Jørgensen, L. B., Malte, H., Ørsted, M., Klahn, N. A., & Overgaard, J. (2021). A unifying model to
700 estimate thermal tolerance limits in ectotherms across static, dynamic and fluctuating exposures to
701 thermal stress. *Scientific Reports*, *11*(1), 12840.
702
703 Jørgensen, L. B., Ørsted, M., Malte, H., Wang, T., & Overgaard, J. (2022). Extreme escalation of
704 heat failure rates in ectotherms with global warming. *Nature*, *611*(7934), 93-98.
705
706 Keefover-Ring, K. (2022). The chemical biogeography of a widespread aromatic plant species shows
707 both spatial and temporal variation. *Ecology and Evolution*, *12*(9).
708

709 Keefover-Ring, K., Ahnlund, M., Abreu, I. N., Jansson, S., Moritz, T., & Albrectsen, B. R. (2014).
710 No evidence of geographical structure of salicinoid chemotypes within Populus tremula. *PLoS*
711 *One*, *9*(10), e107189.
712
713 Kessler, A., & Kalske, A. (2018). Plant secondary metabolite diversity and species
714 interactions. *Annual Review of Ecology, Evolution, and Systematics*, *49*(1), 115-138.
715
716 Kesselmeier, J., & Staudt, M. (1999). Biogenic volatile organic compounds (VOC): an overview on
717 emission, physiology and ecology. *Journal of atmospheric chemistry*, *33*, 23-88.
718
719 Knight, C. A., & Ackerly, D. D. (2002). An ecological and evolutionary analysis of photosynthetic
720 thermotolerance using the temperature-dependent increase in fluorescence. *Oecologia*, *130*(4), 505-
721 514.
722
723 Knight, C. A., Ackerly, D. D. (2003). Evolution and plasticity of photosynthetic thermal tolerance,
724 specific leaf area and leaf size: congeneric species from desert and coastal environments. *New*
725 *Phytologist*. 160: 337–347.
726
727 Loreto, F., Förster, A., Dürr, M., Csiky, O., & Seufert, G. (1998). On the monoterpene emission under
728 heat stress and on the increased thermotolerance of leaves of Quercus ilex L. fumigated with selected
729 monoterpenes. *Plant, Cell & Environment*, *21*(1), 101-107.
730

731 Loreto, F., & Velikova, V. (2001). Isoprene produced by leaves protects the photosynthetic apparatus
732 against ozone damage, quenches ozone products, and reduces lipid peroxidation of cellular
733 membranes. *Plant Physiology*, *127*(4), 1781-1787.
734
735 McCormick, A. C., Unsicker, S. B., & Gershenzon, J. (2012). The specificity of herbivore-induced
736 plant volatiles in attracting herbivore enemies. *Trends in plant science*, *17*(5), 303-310.
737
738 Mastelić, J., & Jerković, I. (2003). Gas chromatography–mass spectrometry analysis of free and
739 glycoconjugated aroma compounds of seasonally collected Satureja montana L. *Food*
740 *chemistry*, *80*(1), 135-140.
741
742 Milos, M., Radonic, A., Bezic, N., & Dunkic, V. (2001). Localities and seasonal variations in the
743 chemical composition of essential oils of Satureja montana L. and S. cuneifolia Ten. *Flavour and*
744 *fragrance journal*, *16*(3), 157-160.
745
746 Muñoz-Bertomeu, J., Arrillaga, I., & Segura, J. (2007). Essential oil variation within and among
747 natural populations of Lavandula latifolia and its relation to their ecological areas. *Biochemical*
748 *systematics and Ecology*, *35*(8), 479-488.
749
750 Napoli, E. M., Curcuruto, G., & Ruberto, G. (2009). Screening the essential oil composition of wild
751 Sicilian oregano. *Biochemical Systematics and Ecology*, *37*(4), 484-493.
752

753 Ørsted, M., Jørgensen, L. B., & Overgaard, J. (2022). Finding the right thermal limit: a framework to
754 reconcile ecological, physiological and methodological aspects of CTmax in ectotherms. *Journal of*
755 *Experimental Biology*, *225*(19), jeb244514.
756
757 Pham, Q. D., Topgaard, D., & Sparr, E. (2015). Cyclic and linear monoterpenes in phospholipid
758 membranes: phase behavior, bilayer structure, and molecular dynamics. *Langmuir*, *31*(40), 11067-
759 11077.
760
761 Pratt, J. D., Keefover-Ring, K., Liu, L. Y., & Mooney, K. A. (2014). Genetically based latitudinal
762 variation in Artemisia californica secondary chemistry. *Oikos*, *123*(8), 953-963.
763
764 Riedlmeier, M., Ghirardo, A., Wenig, M., Knappe, C., Koch, K., Georgii, E., ... & Vlot, A. C. (2017).
765 Monoterpenes support systemic acquired resistance within and between plants. *The Plant Cell*, *29*(6),
766 1440-1459.
767
768 Ross, J.D., & Sombrero C. (1991). Environmental control of essential oil production in Mediterranean
769 plants. Pages 83–94 in Harborne JB, Tomas-Barberan FA, eds. Ecological Chemistry and
770 Biochemistry of Plant Terpenoids. Oxford: Clarendon Press.
771
772 Sáez, F., & Stahl-Biskup, E. (2002). Essential oil polymorphism in the genus Thymus. In *Thyme* (pp.
773 139-157). CRC Press.
774
775 Sastry A., & Barua D. (2017). Leaf thermotolerance in tropical trees from a seasonally dry climate
776 varies along the slow–fast resource acquisition spectrum. *Scientific Reports.* 7: 11246.

Seemann, J. R., Berry, J. A., & Downton, W. J. S. (1984). Photosynthetic response and adaptation to high temperature in desert plants: a comparison of gas exchange and fluorescence methods for studies of thermal tolerance. *Plant Physiology*, *75*(2), 364-368.

Sharkey, T. D., & Singsaas, E. L. (1995) Why plants emit isoprene. *Nature*, 374: 769

Su, J., Wang, Y., Bai, M., Peng, T., Li, H., Xu, H. J., ... & Wu, H. (2023). Soil conditions and the plant microbiome boost the accumulation of monoterpenes in the fruit of Citrus reticulata 'Chachi'. *Microbiome*, *11*(1), 61.

Thompson, J. D. (2020). *Plant evolution in the Mediterranean: insights for conservation*. Oxford University Press.

Thompson, J., Charpentier, A., Bouguet, G., Charmasson, F., Roset, S., Buatois, B., ... & Gouyon, P. H. (2013). Evolution of a genetic polymorphism with climate change in a Mediterranean landscape. *Proceedings of the National Academy of Sciences*, *110*(8), 2893-2897.

Thompson, J. D., Gauthier, P., Amiot, J., Ehlers, B. K., Collin, C., Fossat, J., ... & Linhart, Y. B. (2007). Ongoing adaptation to Mediterranean climate extremes in a chemically polymorphic plant. *Ecological Monographs*, *77*(3), 421-439.

799 Thompson, J. D., Rolland, A. G., & Prugnolle, F. (2002). Genetic variation for sexual dimorphism in
800 flower size within and between populations of gynodioecious Thymus vulgaris. *Journal of*
801 *Evolutionary Biology*, *15*(3), 362-372.
802
803 Tian, Z., Luo, Q., Li, Y., & Zuo, Z. (2020). Terpinene and β-pinene acting as signaling molecules to
804 improve Cinnamomum camphora thermotolerance. *Industrial Crops and Products*, *154*, 112641.
805
806 Vernet, P., Gouyon, R. H., & Valdeyron, G. (1986). Genetic control of the oil content in Thymus
807 vulgaris L: a case of polymorphism in a biosynthetic chain. *Genetica*, *69*(3), 227-231.
808
809 Vernet, P., Guillerm, J.L., Gouyon, P. H. (1977). Le polymorphisme chimique de Thymus vulgaris
810 L. (Labiée) I. Repartition des formes chimiques en relation avec certains facteurs écologiques. *Oecol*
811 *Plant*, 12(2), 159–179.
812
813 Walker, T. W., Alexander, J. M., Allard, P. M., Baines, O., Baldy, V., Bardgett, R. D., ... & Salguero-
814 Gómez, R. (2022). Functional Traits 2.0: The power of the metabolome for ecology. *Journal of*
815 *Ecology*, *110*(1), 4-20.
816
817 Wenig, M., Ghirardo, A., Sales, J. H., Pabst, E. S., Breitenbach, H. H., Antritter, F., ... & Vlot, A. C.
818 (2019). Systemic acquired resistance networks amplify airborne defense cues. *Nature*
819 *communications*, *10*(1), 3813.
820

Willits, D. H., & Peet, M. M. (2001). Measurement of chlorophyll fluorescence as a heat stress indicator in tomato: laboratory and greenhouse comparisons. *Journal of the American Society for Horticultural Science*, *126*(2), 188-194.

Wood, S. N. (2017). Generalized additive models: an introduction with R. Boca Raton, FL, USA: CRC Press.

Xu, C., Wang, B., Luo, Q., Ma, Y., Zheng, T., Wang, Y., ... & Zuo, Z. (2022). The uppermost monoterpenes improving Cinnamomum camphora thermotolerance by serving signaling functions. *Frontiers in Plant Science*, *13*, 1072931.

Zhao, M., Wang, L., Wang, J., Jin, J., Zhang, N., Lei, L., ... & Song, C. (2020). Induction of priming by cold stress via inducible volatile cues in neighboring tea plants. *Journal of Integrative Plant Biology*, *62*(10), 1461-1468.

Zielińska-Błajet, M., & Feder-Kubis, J. (2020). Monoterpenes and their derivatives—Recent development in biological and medical applications. *International Journal of Molecular Sciences*, *21*(19), 7078.

Zuo, Z., Wang, B., Ying, B., Zhou, L., & Zhang, R. (2017). Monoterpene emissions contribute to thermotolerance in Cinnamomum camphora. *Trees*, *31*, 1759-1771.

Supplementary material

Article title: The scent of survival in a warming world: how monoterpenes drive thermal adaptation in thyme

The following Supporting Information is available for this article:

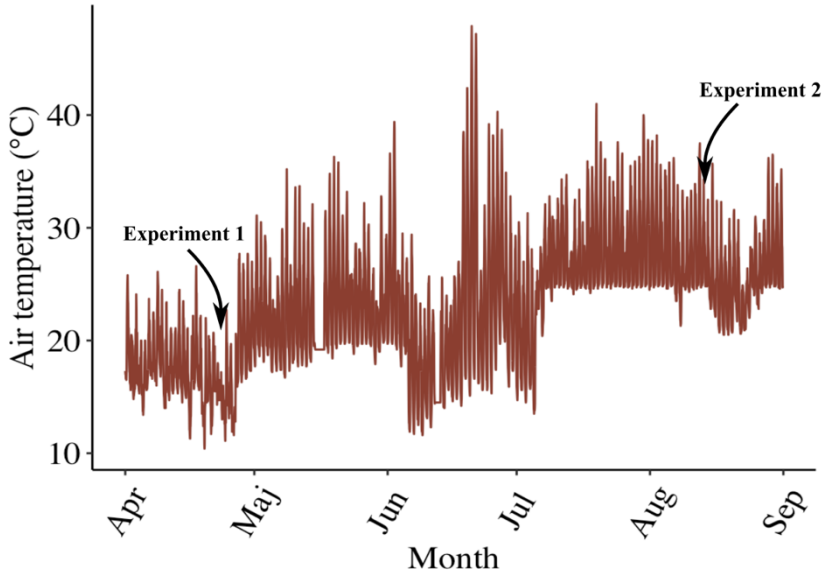

Figure S1. Greenhouse temperature conditions during the growth of *Thymus vulgaris* plants used for thermal tolerance experiments. Plants were grown under controlled winter-like conditions from December 2023 to March 2024 where daily temperatures were maintained between approximately 5 and 20 °C to simulate Mediterranean winter conditions. The first thermal tolerance experiment was conducted in April 2024, when all plants were flowering and temperatures ranged from ~13 to 20 °C. After this experiment, greenhouse temperatures were allowed to follow ambient conditions, gradually increasing with the season. The second thermal tolerance experiment was conducted in mid-August 2024, under summer-like conditions with daily temperatures ranging between 25 and 35 °C.

Figure S2. Thermal failure times for all heat stress experiments used in this study to generate chemotype specific TDT models. Generalized additive models (GAMs) were fitted to the maximum quantum efficiency (F_v/F_m) of PSII as a function of stress duration for each assay. The fitted GAMs (black lines) show the estimated decrease in F_v/F_m, and vertical dashed lines indicate the time point at which F_v/F_m dropped by 50%, defining the time of thermal failure. The individual assays are labelled according to their chemotype and stress intensity in April (44, 45, 46, 47 and 48 °C) and in August (44, 45, 46, 47, 48 and 49 °C). These temperatures correspond to labels **A**, **B**, **C**, **D**, and **E** for April, and **A**, **B**, **C**, **D**, **E**, and **F** for August.

Heat stress experiment – April 2024

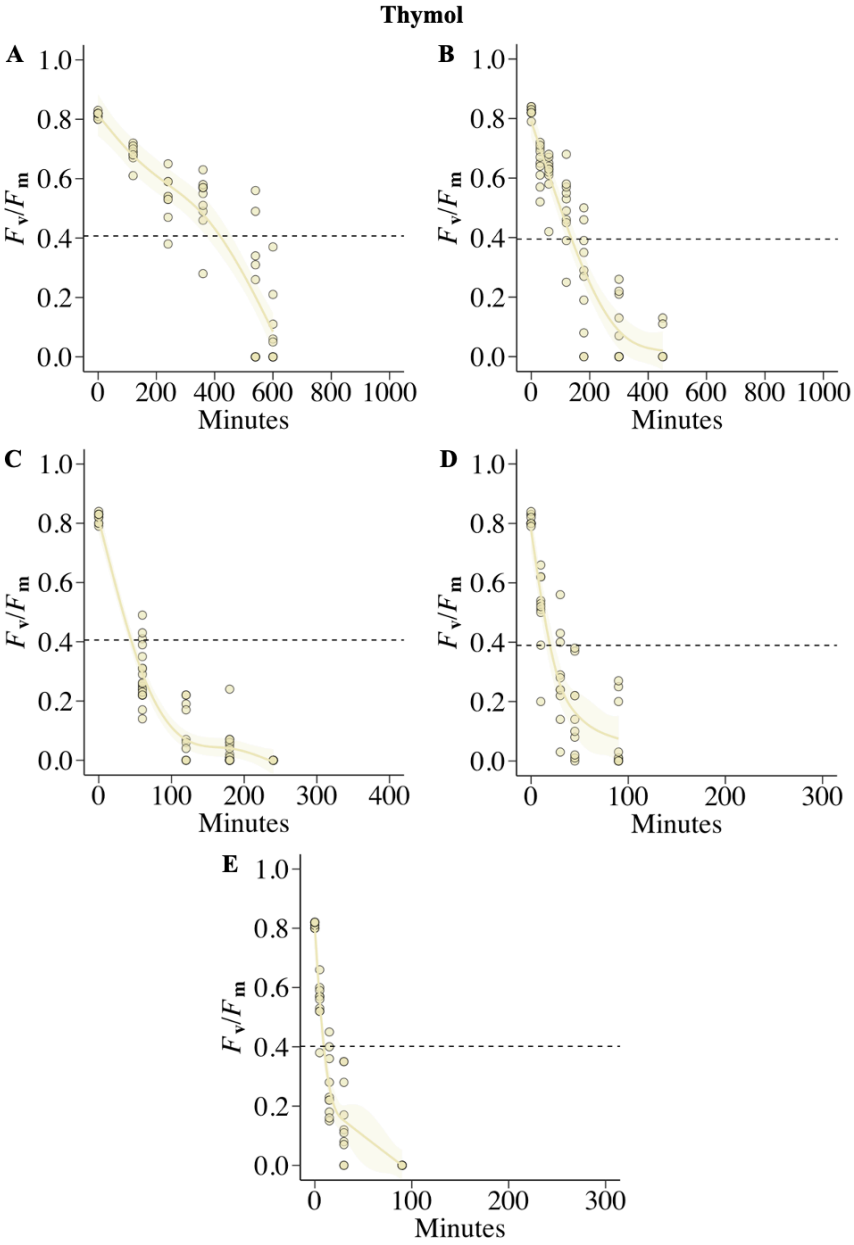

877

878

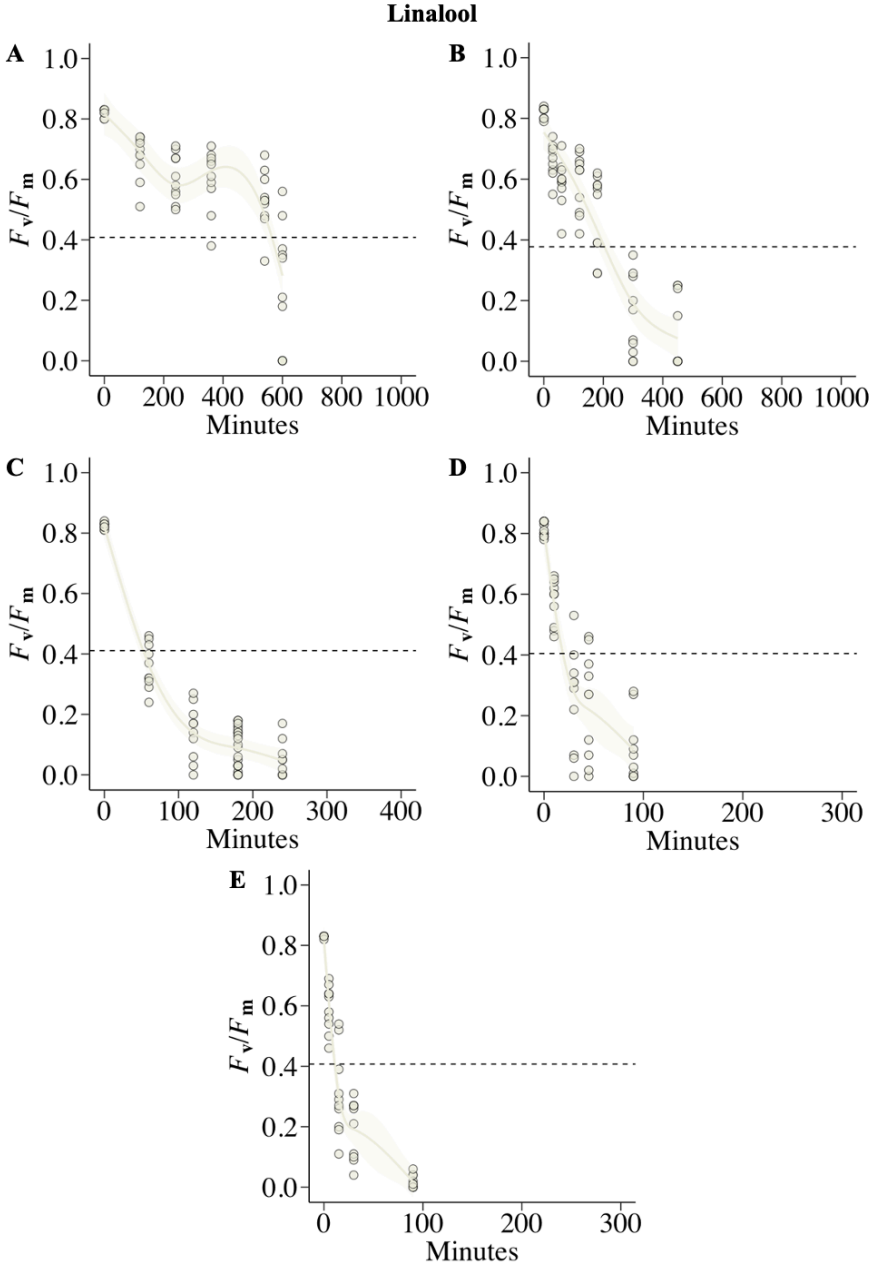

879

880

881

882

883

884

885

886

887

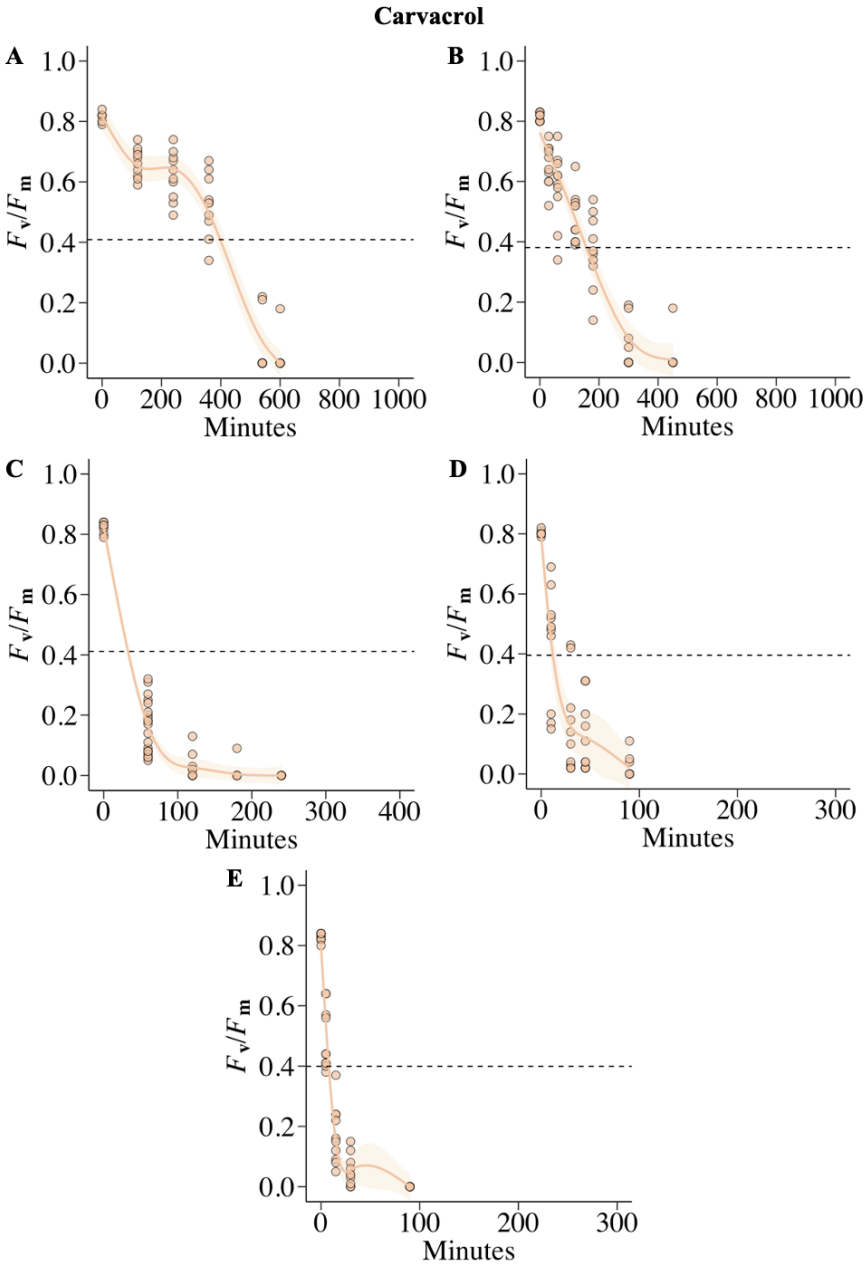

888

889

890

891

892

893

894

895

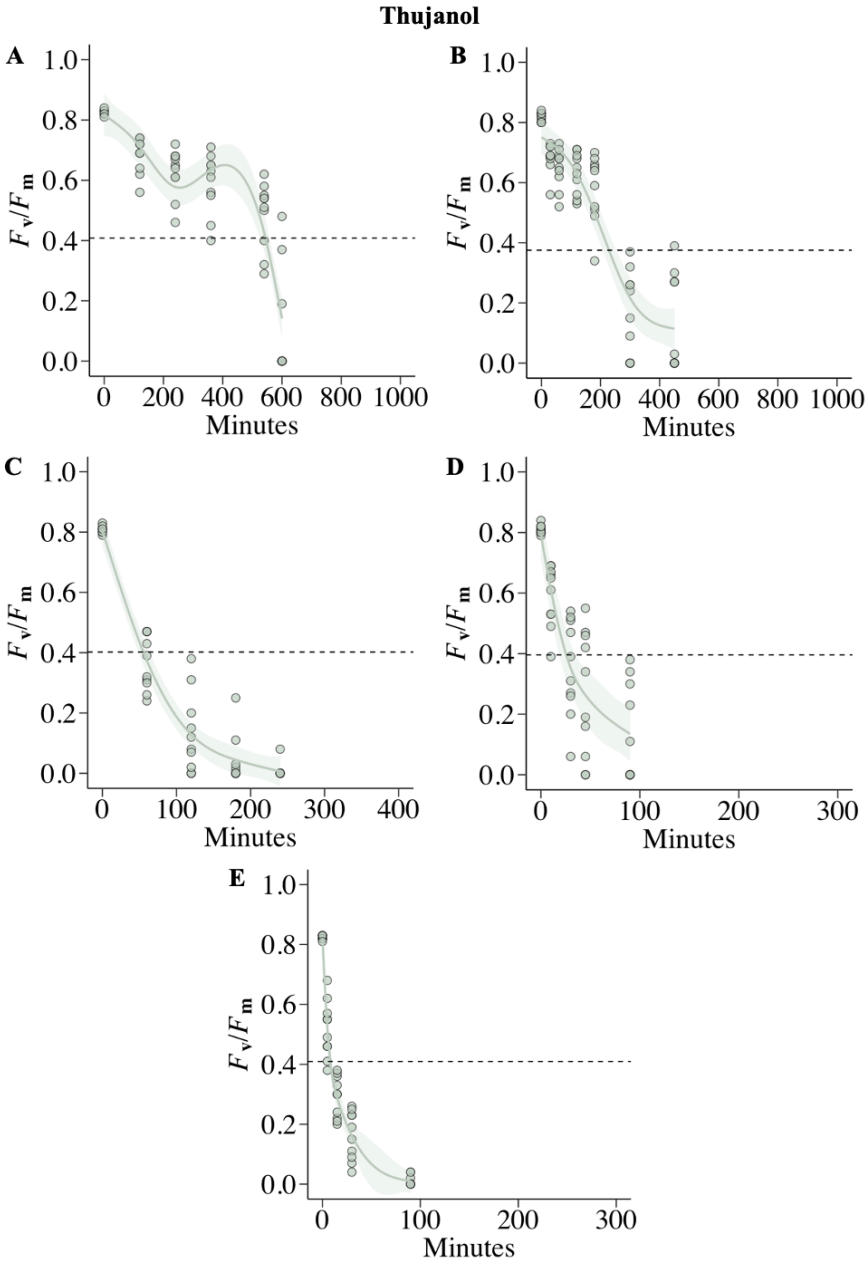
Thujanol
A
B
C
D
E
F_v/F_m
Minutes
0.0
0.2
0.4
0.6
0.8
1.0
0
100
200
300
400
600
800
1000

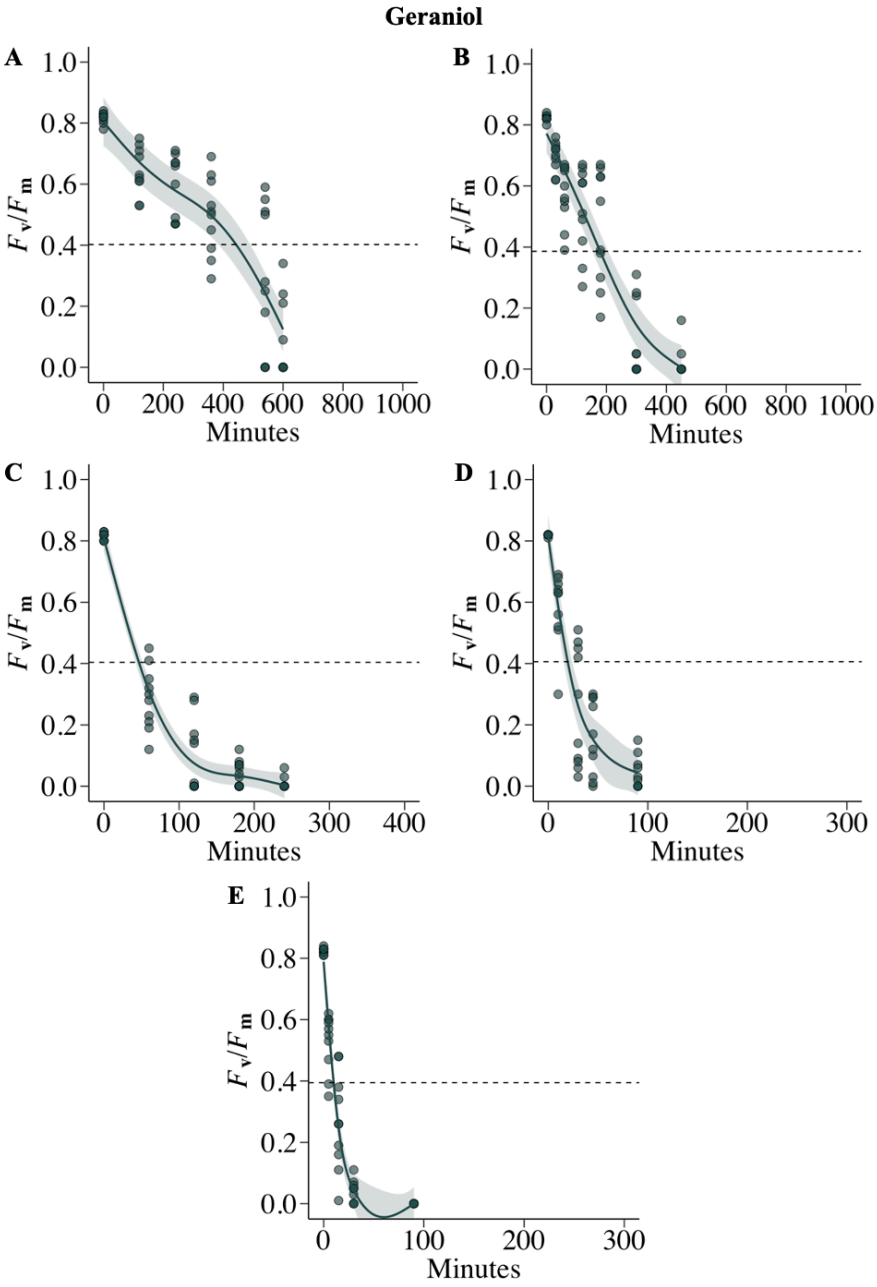

906

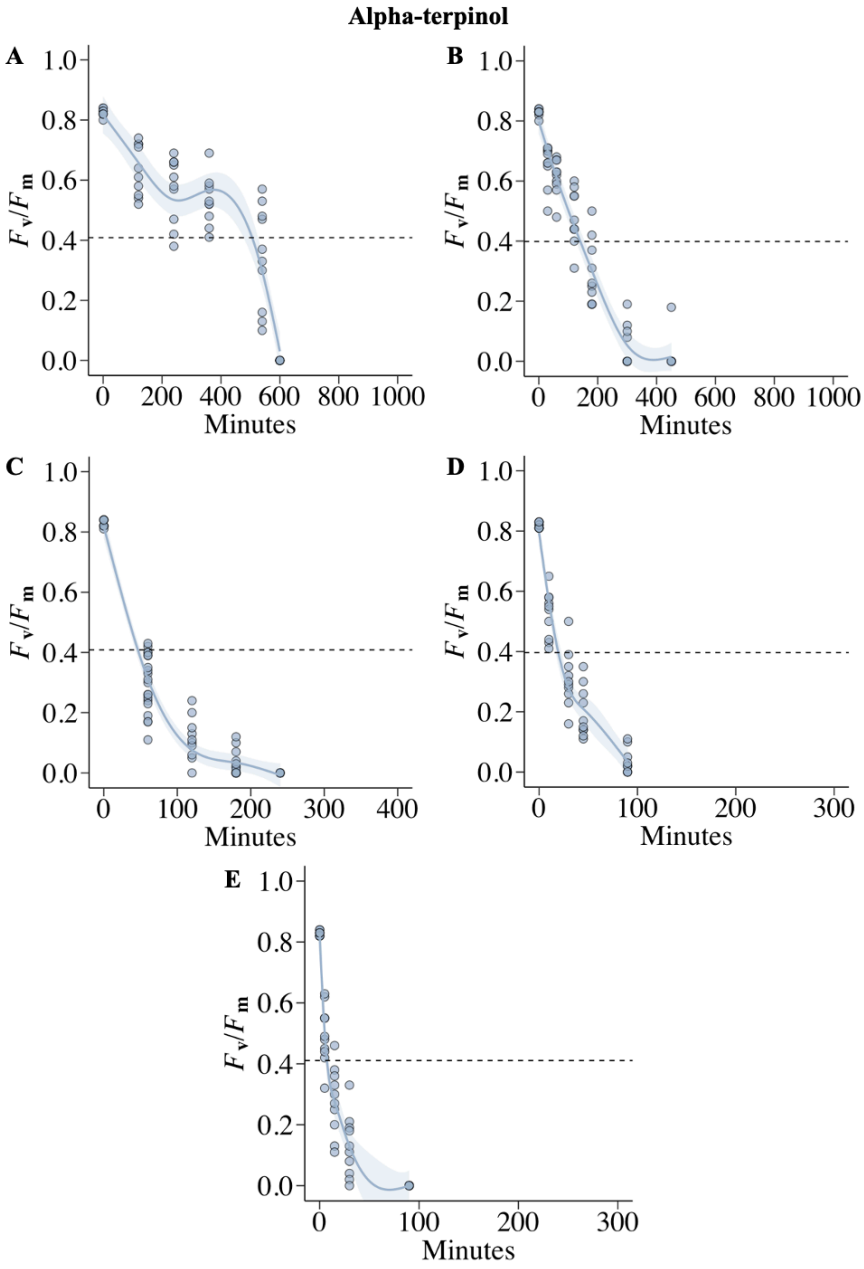
Alpha-terpinol
A
B
C
D
E
F_v/F_m
Minutes
0.0
0.2
0.4
0.6
0.8
1.0
0
100
200
300
400
600
800
1000

Heat stress experiment – August 2024

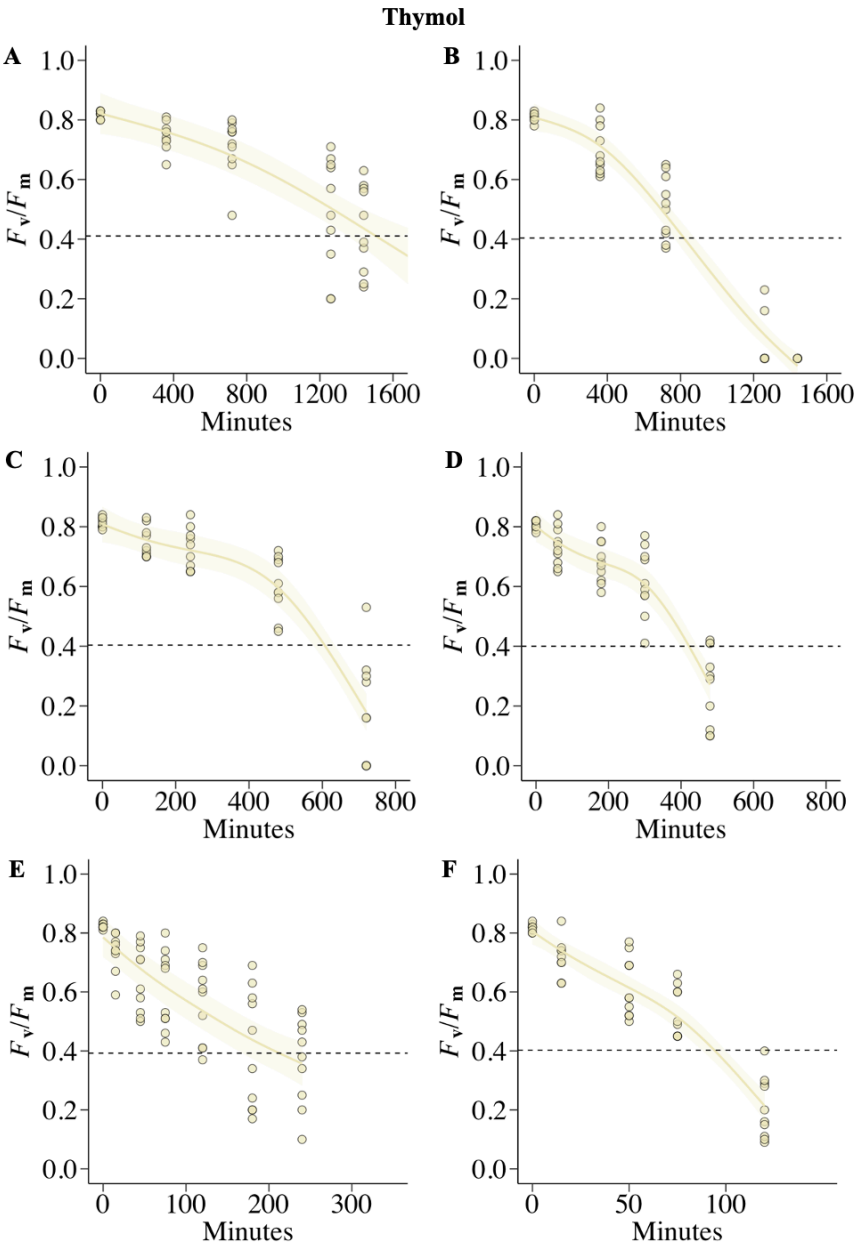

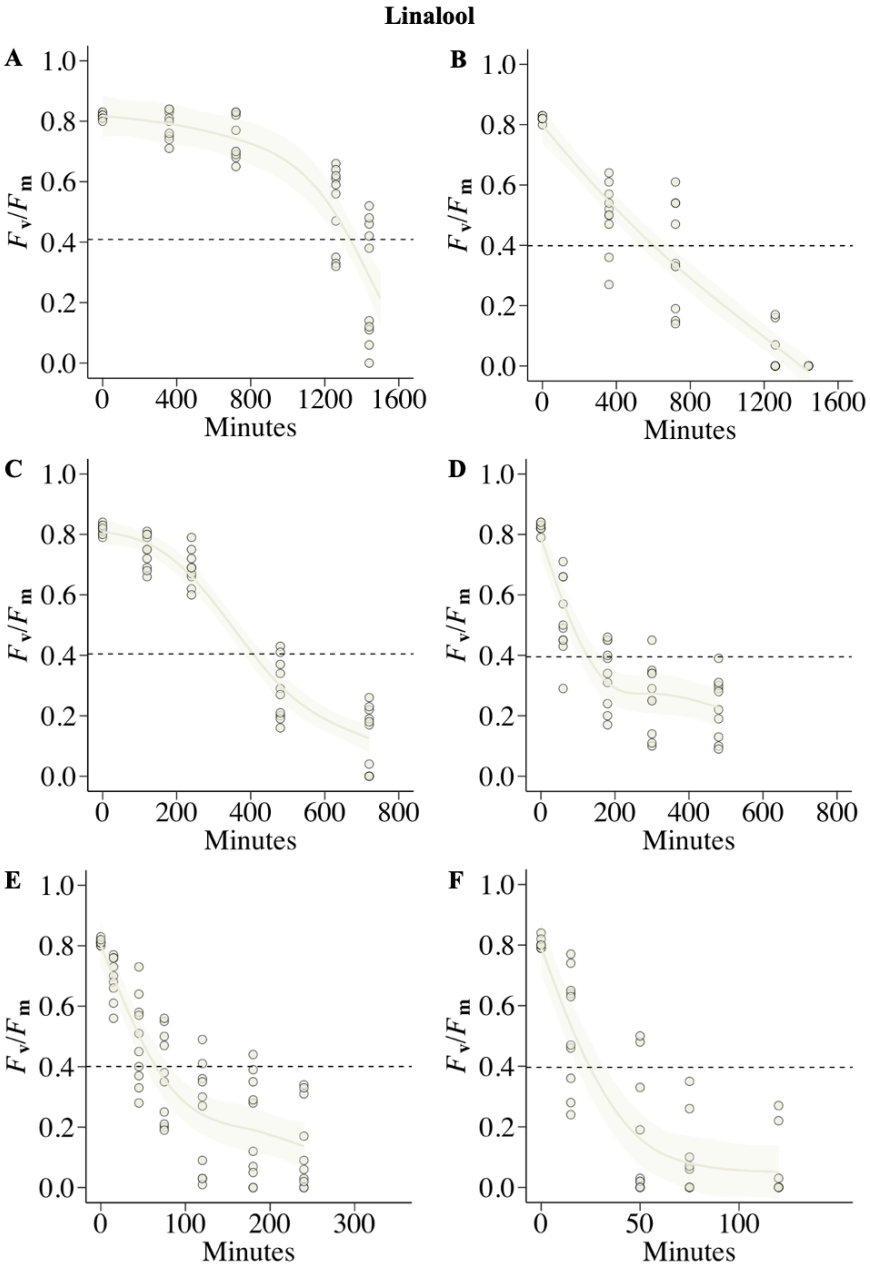
Linalool
A
B
C
D
E
F
F_v/F_m
Minutes
0.0
0.2
0.4
0.6
0.8
1.0
0
400
800
1200
1600
200
600
100
300
50

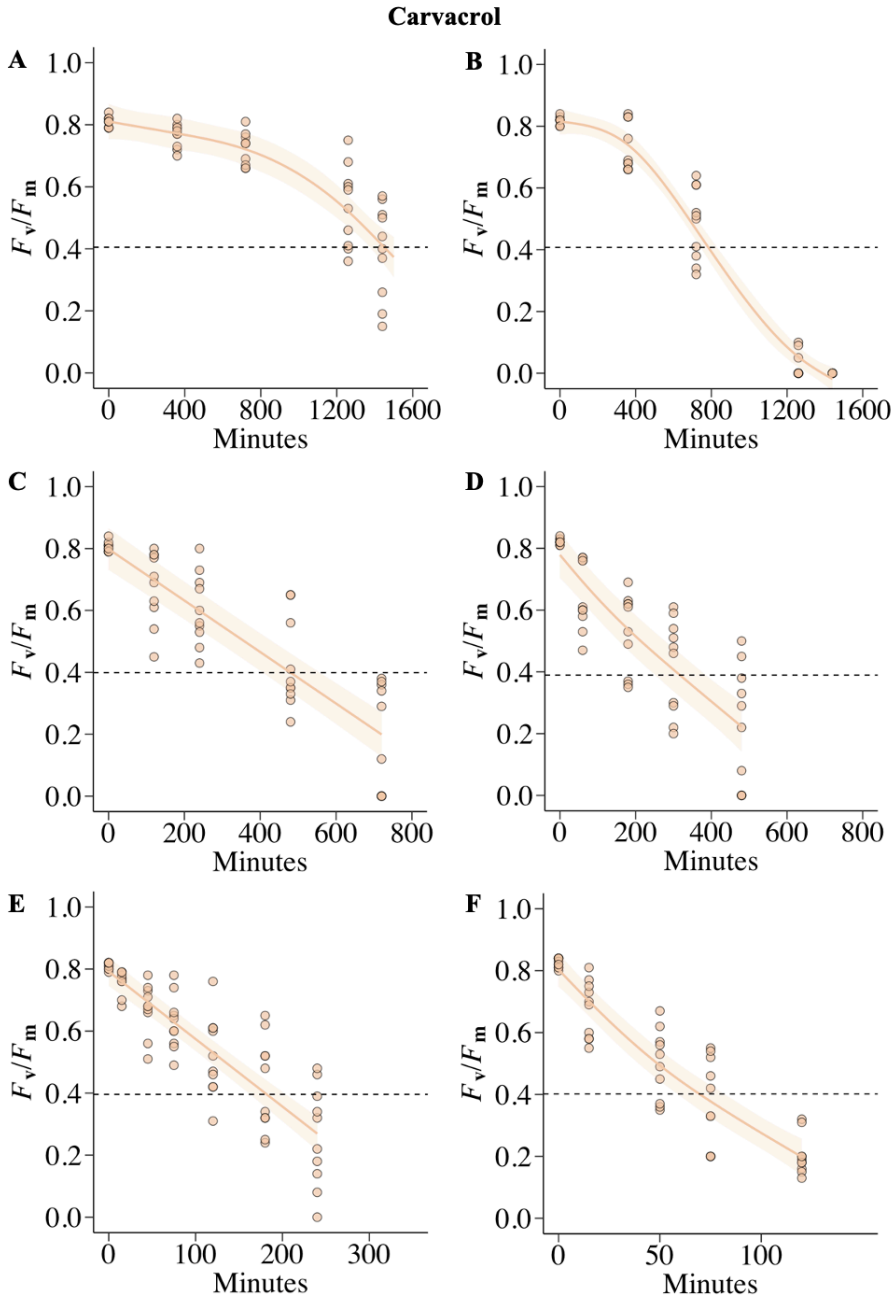

931
932
933
934
935
936
937
938

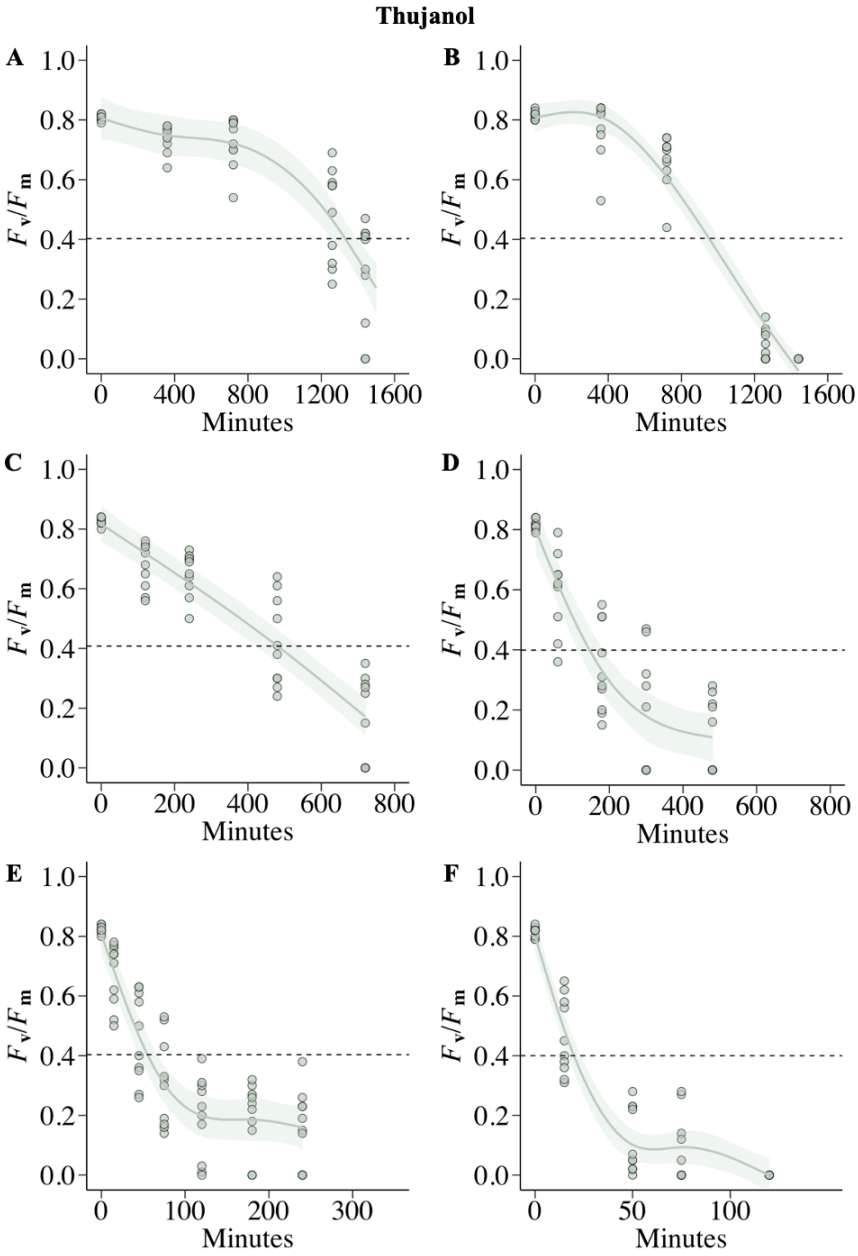
Thujanol
A
B
C
D
E
F
F_v/F_m
Minutes
0.0
0.2
0.4
0.6
0.8
1.0
0
400
800
1200
1600
200
600
100
300
50

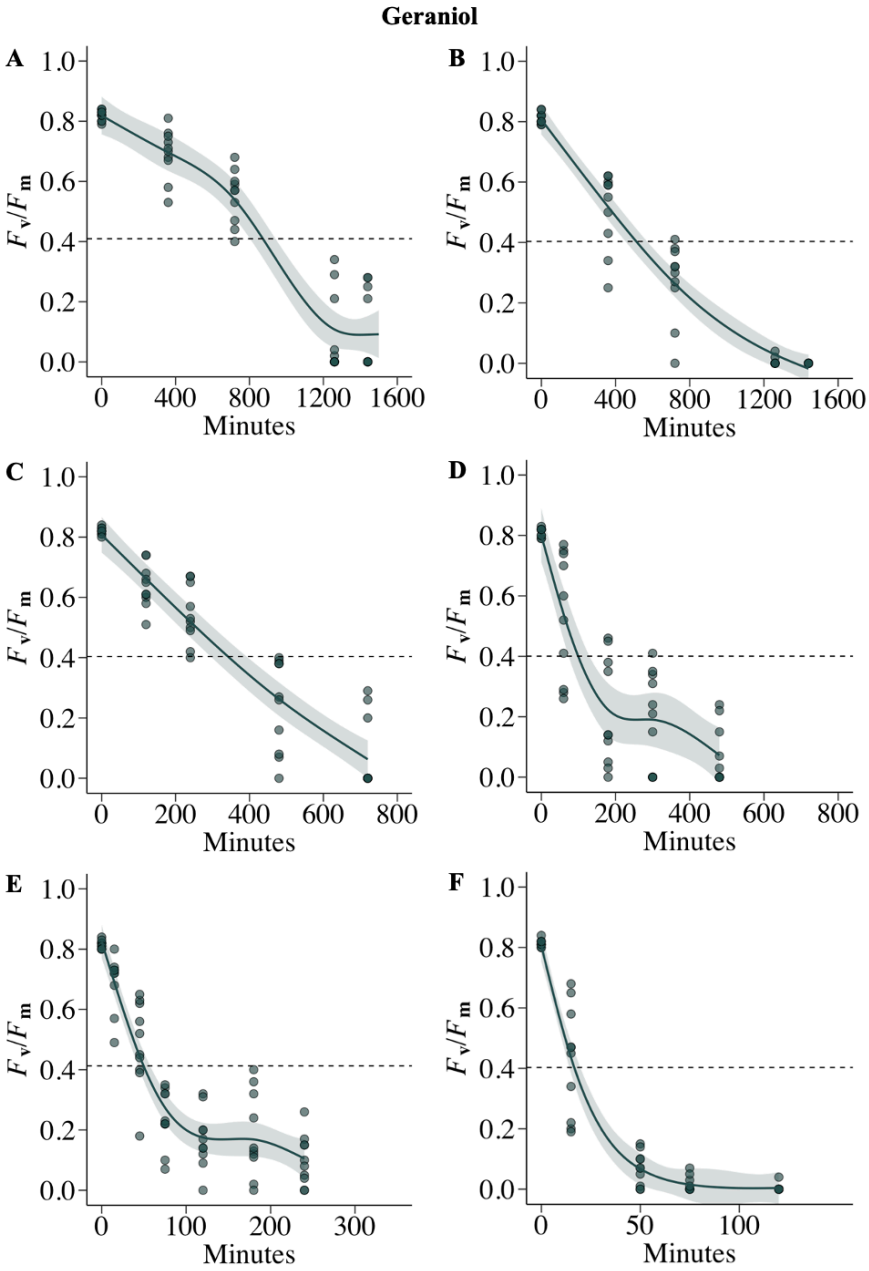
Geraniol
A
B
C
D
E
F
F_v/F_m
Minutes
0.0
0.2
0.4
0.6
0.8
1.0
0
400
800
1200
1600
200
600
100
300
50

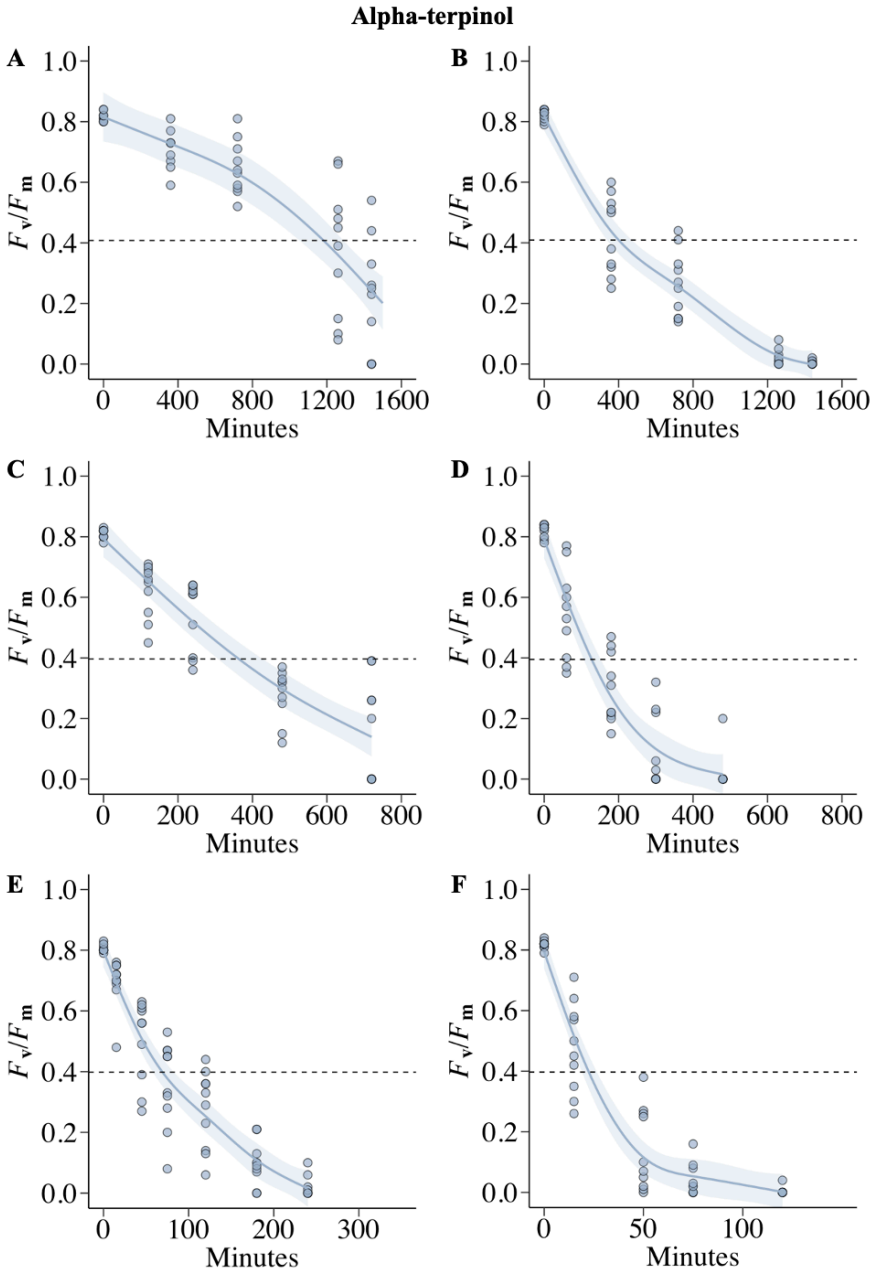
Alpha-terpinol
A
B
C
D
E
F
F_v/F_m
Minutes

Figure S3. Diurnal field measurements of leaf physiological parameters in *Thymus vulgaris* across site types from St. Martin de Londres, southern France, in June 2024. Sites were categorized into site types based on whether the *Thymus vulgaris* population was predominantly phenolic, non-phenolic, or mixed (i.e., roughly equal proportions of phenolic and non-phenolic individuals). Panels show **A**) leaf net photosynthesis (µmol CO_2 m^{-2} s^{-1}), **B**) leaf dark respiration (µmol CO_2 m^{-2} s^{-1}), **C**) leaf transpiration (mm H_2O m^{-2} s^{-1}), **D**) maximum quantum efficiency of photosystem II (F_v/F_m), and **E**) effective quantum efficiency of photosystem II (F_v'/F_m'). Measurements were conducted between approximately 11:00 and 16:00 under ambient light conditions. Leaf temperature during the gas-exchange measurement was set to the temperature measured on the leaf with a thermocouple immediately before clamping the gas-exchange chamber.